Advanced Drug Delivery Reviews 174 (2021) 250–264

Contents lists available at ScienceDirect

Advanced Drug Delivery Reviews

journal homepage: www.elsevier.com/locate/adr

Illuminating RNA trafficking and functional delivery by extracellular vesicles

Willemijn S. de Voogt [a], Marvin E. Tanenbaum [b], Pieter Vader [a,c,*]

[a] CDL Research, University Medical Center Utrecht, Heidelberglaan 100, 3584 CX Utrecht, the Netherlands
[b] Oncode Institute, Hubrecht Institute-KNAW and University Medical Center, Uppsalalaan 8, 3584 CT Utrecht, Utrecht, the Netherlands
[c] Department of Experimental Cardiology, University Medical Center Utrecht, Heidelberglaan 100, 3584 CX Utrecht, the Netherlands

ARTICLE INFO

Article history:
Received 29 January 2021
Revised 7 April 2021
Accepted 17 April 2021
Available online 21 April 2021

Keywords:
Extracellular vesicles
Exosomes
RNA-based therapeutics
FISH
Live-cell imaging
CRISPR/Cas
Molecular beacon
MS2-system
Fluorogenic aptamer

ABSTRACT

RNA-based therapeutics are highly promising for the treatment of numerous diseases, by their ability to tackle the genetic origin in multiple possible ways. RNA molecules are, however, incapable of crossing cell membranes, hence a safe and efficient delivery vehicle is pivotal. Extracellular vesicles (EVs) are endogenously derived nano-sized particles and possess several characteristics which make them excellent candidates as therapeutic RNA delivery agent. This includes the inherent capability to functionally transfer RNAs in a selective manner and an enhanced safety profile compared to synthetic particles. Nonetheless, the fundamental mechanisms underlying this selective inter- and intracellular trafficking and functional transfer of RNAs by EVs are poorly understood. Improving our understanding of these systems is a key element of working towards an EV-based or EV-mimicking system for the functional delivery of therapeutic RNA. In this review, state-of-the-art approaches to detect and visualize RNA *in situ* and in live cells are discussed, as well as strategies to assess functional RNA transfer, highlighting their potential in studying EV-RNA trafficking mechanisms.

© 2021 The Author(s). Published by Elsevier B.V. This is an open access article under the CC BY-NC-ND license (http://creativecommons.org/licenses/by-nc-nd/4.0/).

Contents

Abbreviations: AiFC, Aptamer-initiated fluorescence complementation; Cas, CRISPR associated endonuclease; CHARGE, Catalytic hairpin assembly RNA circuit; CRISPR, Clustered regulatory interspaced palindromic repeat; ddPCR, Digital droplet PCR; DMHBI, 3,5-dimethoxy-4-hydroxybenzylidene imidazolinone; EV, Extracellular vesicle; FISSEQ, Fluorescence *in situ* sequencing; FISH, Fluoresence *in situ* hybridization; FP, Fluorescent protein; HCR, Hybridization chain reaction; MB, Molecular beacon; MERFISH, Multiplexed error robust FISH; MBS, MS2 binding site; MCP, MS2 bacteriophage coat protein; NLS, Nuclear localization signal; PAM, Protospacer adjacent motif; PCR, Polymerase chain reaction; PCP, PP7 bacteriophage coat protein; RT-qPCR, Reverse transcription quantitative PCR; SeqFISH, Sequential FISH; SLO, Streptolysin O; smFISH, single-molecule FISH; SMLM, Single-molecule localization microscopy; SNR, Signal-to-noise ratio.

* Corresponding author at: Central Diagnostic Laboratory and Department of Experimental Cardiology, Heidelberglaan 100, 3584 CX Utrecht, the Netherlands.
E-mail addresses: w.s.devoogt-2@umcutrecht.nl (W.S. de Voogt), m.tanenbaum@hubrecht.eu (M.E. Tanenbaum), pvader@umcutrecht.nl (P. Vader).

https://doi.org/10.1016/j.addr.2021.04.017
0169-409X/© 2021 The Author(s). Published by Elsevier B.V.
This is an open access article under the CC BY-NC-ND license (http://creativecommons.org/licenses/by-nc-nd/4.0/).

1. Introduction

RNA-based therapeutics hold great potential for the treatment of many diseases, including cancer and a variety of neurological disorders. Uniquely, they have the ability to specifically silence genes (siRNA and miRNA), express genes (mRNA) or edit genes (sgRNA in combination with Cas9 protein or mRNA) [1,2]. Effective and safe delivery of RNA-based drugs, however, remains challenging due to several factors. (i) Naked unmodified RNA molecules are not capable of independently crossing biological membranes due to their size and negative charge. (ii) They are susceptible to degradation by RNases and are rapidly cleared by the kidneys and liver. (iii) RNAs are ligands of several toll-like receptors and can, therefore, activate a strong innate immune response [3]. To overcome these limitations, materials that can assist safe and effective intracellular delivery of RNAs are widely studied. Such delivery vehicles can, for example, encapsulate or complex RNA, thereby hiding it for RNases and the immune system. A prerequisite for therapeutic efficacy is that the carrier, when internalized in the target cells via endocytic pathways, must be able to escape degradation in the endolysosomal pathway. This endosomal escape results in the functional release of the RNA into the cytosol where RNA carries out its biological effect in the recipient cells [2]. The applications of various synthetic delivery vehicles have been investigated, including, for instance, peptides [4], polymer-based nanoparticles [5] and lipid-based nanoparticles [6]. Nonetheless, their immunogenicity is a major concern. Furthermore, most of these delivery systems consist of positively charged molecules to complex the polyanionic RNA molecules. Their cationic groups, however, are associated with cytotoxicity [7,8]. Furthermore, endosomal escape is still an inefficient process and the applications of these synthetic nanoparticles beyond targeting the liver are limited [3,9]. Exploiting endogenous nanocarriers for RNA delivery may result in less immunogenicity and cytotoxicity compared to synthetic particles [10]. Besides, natural delivery vehicles may contain inherent properties that allow more efficient uptake, endosomal escape and thereby functional RNA delivery [11].

Extracellular vesicles (EVs) are cell-derived vesicles that can be classified according to their biogenesis into exosomes, microvesicles or apoptotic bodies. Exosomes originate from the endocytic pathway as intraluminal vesicles, which are formed by inward budding within multivesicular bodies. They are released from the cell upon fusion of the multivesicular body with the plasma membrane. The size of exosomes ranges from approximately 30 nm to 120 nm. In contrast, EVs that are directly formed by budding from the plasma membrane are called microvesicles (or ectosomes), which are more heterogeneous in size (50 nm – 1 μm). Apoptotic bodies range in size from 50 nm to 2 μm and are formed by outward budding of apoptotic cells [12]. Due to the overlap in size between EV populations and the lack of consensus on subtype-specific EV markers, experimentally demonstrating the intracellular origin of EVs after their release is challenging. Therefore, more recently, it is encouraged to classify the particles as small or large EVs or according to their biochemical composition [13,14]. Initially, EVs were described as cellular "waste bins" that eliminate all unneeded material from the cells. However, in 2006 it was first reported that EVs may be capable of functionally transferring mRNA, as incubation of embryonic stem cell EVs containing Oct-4 mRNA with SKL cells resulted in mRNA delivery to the target cells [15]. Shortly after, these results were confirmed by the demonstration that mouse mast cell EVs (obtained through 0.22 μm filtration followed by ultracentrifugation at 120,000g) functionally transferred mRNA to other mast cells [16]. It is now known that EVs facilitate intercellular communication by exchanging cargo, including proteins, nucleic acids, and lipids, between cells [17,18]. These findings have resulted in a rapidly expanding research field that focuses on exploiting EVs as natural nanoparticles for therapeutic RNA delivery purposes, as they may assist to overcome the issues involved in utilizing synthetic particles.

Methods to load RNAs in EVs can be divided into loading before or after EV isolation. Loading before isolation may be established by transfection of the EV donor cells with RNA or by stable RNA expression in an engineered cell line and subsequent production and release of EVs encapsulating the RNA. RNA loading after isolation can be performed by electroporation, sonication or extrusion [9]. Numerous studies already reported *in vivo* functional delivery of exogenous RNA by EVs derived from various cell types loaded after EV isolation [19–21], highlighting the enormous potential of EVs as an RNA drug carrier. However, it should be considered that these loading methods may alter the structure and activity of EVs and their RNA cargo. Loading before isolation better resembles natural RNA loading, however, the observed loading efficiencies are relatively low [9]. To improve loading, comprehending the mechanisms regulating cargo sorting is essential. Some crucial questions regarding the RNA cargo sorting remain to be answered. For instance, what cellular factors drive RNA loading into the EV lumen and to what extent does this depend on RNA sequence or structure? And is sorting affected by the subcellular localization of RNAs [22]?

Once released by donor cells, EVs must be internalized in target cells followed by intracellular RNA delivery to become efficacious. Several endocytic pathways have been suggested to be responsible for the uptake of EVs in the recipient cells, a process that might be dependent on the recipient cell-type. Afterwards, how EVs escape lysosomal degradation and release functional RNA intracellularly remains largely unexplored. For instance, RNA release might be dependent on the route of EV uptake [23,24]. Learning the fate of EVs and the RNA in recipient cells is crucial in developing efficacious EV-based RNA therapies.

Besides subdividing EVs into different subtypes, evidence also points towards the existence of subpopulations within exosomes and microvesicles with distinct biological characteristics, adding to the complexity of EV communication mechanisms [25,26]. The extent of heterogeneity in RNA cargo and the biological effects in recipient cells upon functional RNA delivery between EVs derived from different cell types, or even within subpopulations of EVs released from the same cells, remains largely unknown. For instance, a recent study demonstrates that subpopulations of EVs with distinct surface marker expression are also enriched in distinct miRNA populations [27]. This implies that selective pathways of RNA packaging exist, resulting in the release of functionally diverse subpopulations of EVs. Interestingly, small non-coding RNAs are the main RNA cargo species in EVs, although mRNA and lncRNAs are found as well [28–30]. Even for the most abundant miRNA species, however, the calculated average copy number per EV in pools derived from various cell sources is less than 1 [31]. Together with an increasing number of studies that have shown physiological effects upon EV-RNA delivery, this suggests that

EV-RNA delivery must be highly effective or specific. Comprehending EV subpopulations to gain insight into the optimal subpopulation for RNA trafficking and functional delivery to specific target cells could increase the overall performance of EVs as delivery vehicles for RNA. In summary, to optimize the therapeutic ability of RNA delivery by EVs, an in-depth understanding of the biological processes underlying RNA cargo sorting and trafficking, both inter- and intracellular, is pivotal.

Direct RNA visualization can provide crucial information on the localization of RNA content within an EV or cell. Moreover, live-cell imaging can increase our understanding of the dynamics of RNA sorting and trafficking by EVs. Visualizing and tracking RNA is essential to investigate the biological processes underlying cargo sorting and EV-mediated intra- and intercellular trafficking. This may improve the application of EVs as RNA nanocarriers. In addition, sensitive assessment methods for the functional delivery of RNA to target cells by EVs are crucial. Several elegant approaches are established to image EVs [32]. In contrast, sensitive methods to track the RNA content of EVs spatially and temporally are limited. Taking the limited number of RNA copies in EVs into account, highly sensitive and preferably single-molecule detection methods are required. This review will provide an overview of techniques that are currently used to detect EV-RNA. In addition, newly developed approaches for RNA imaging in fixed tissue and live cells and their potential for EV-RNA visualization will be discussed. Moreover, available methods to study functional transfer of EV-RNA will be discussed.

2. Current techniques to detect EV-RNA

When discussing intracellular RNA detection techniques, techniques that provide information on RNA quantity and techniques that also enable RNA visualization can be distinguished. Presently, detecting RNA in EVs is mostly limited to quantifying specific RNAs in EV populations or recipient tissues rather than in single EVs or cells. In this chapter, the most commonly-used RNA quantification methods will be discussed, as well as the various approaches that have been used to visualize EV-RNA.

2.1. Quantitative EV-RNA detection

The most well-established technique to detect RNA in EVs is reverse transcription quantitative PCR (RT-qPCR). It provides quantitative information on the levels of individual transcripts and can therefore be employed for the determination of RNA expression levels within cell or EV populations. The basic principle of this technique is to synthesize cDNA by reverse transcriptase, which is then used as a template for the qPCR reaction. Hereby, labeling of the amplified DNA with a specific dye enables transcript quantification relative to a measured reference gene [33]. RT-qPCR is among the most sensitive RNA quantification methods and is currently the gold standard for studying RNA levels in EVs [34].

Droplet digital PCR (ddPCR) is a relatively new PCR technique that can be utilized for absolute quantification of RNA without the requirement of normalization to reference transcripts, in contrast to RT-qPCR. Moreover, it is suitable for high-throughput screening. ddPCR relies on generating sample-in-oil droplets that are transferred to a PCR plate. After amplification, droplet fluorescence can be measured. Each droplet emits a fluorescent signal with a unique intensity, which can be assigned as positive or negative by applying a certain threshold. This enables absolute quantification [35]. It has been demonstrated using ddPCR that miRNAs with an abundance of merely 1.4 copies / 10^6 EVs could be detected, indicating that this technique is highly sensitive [36]. In a comparative study, urine EV levels of miRNAs with low, medium or high abundances were measured with RT-qPCR and ddPCR. Using RT-qPCR, the low abundance miRNA-29a (less than 100 copies / μL urine) could not be detected, whereas with ddPCR, an absolute copy number of miRNA-29a between 5 and 50 / μL urine was observed [37].

To investigate expression profiles of total RNA in an EV population, RNA sequencing (RNAseq) is widely employed. Similar to RT-qPCR, this high-throughput sequencing approach relies on isolating total RNA and converting this to cDNA. Rather than using transcript-specific primers, however, sequencing adaptors are ligated to the cDNA enabling amplification and sequencing of total RNA. Optionally, by selecting the isolated total RNA on size or the presence of a poly-A sequence, for instance, sequencing can specifically be performed on small RNA or mRNA species [38]. Using RNAseq, it has been uncovered that EVs derived from various cell types contain mainly small non-coding RNA species rather than intact mRNAs or lncRNAs [28,29].

An important consideration for quantitative EV-RNA detection is the potential detection of RNA contaminants derived from cell culture media. For instance, it has been demonstrated that RNA contaminants derived from FBS can directly influence miRNA expression profiles in EVs when detected by RT-qPCR and RNAseq [39,40]. Furthermore, applying PCR-based techniques for the detection of EV-RNA trafficking has two main limitations. First, distinguishing between EV-derived RNA and endogenous RNA in the recipient cells is challenging. Utilizing EV recipient cells that are isolated from specific RNA knockout mice is an interesting approach to overcome this issue, as this excludes the possibility of detecting this specific endogenous RNA. Following this approach, it has been demonstrated that synthetic miR-155 was delivered by EVs (obtained through 0.4 μm and 0.22 μm filtration followed by CD63-immunocapturing and, after electroporation, ExoQuick-TC™ isolation) into hepatocytes and Kuppfer cells derived from miR-155 knockout mice [41]. Second, these approaches are not sensitive enough to detect EV-RNA in a single EV or recipient cell. Therefore, they are limited to RNA detection in populations of cells or EVs. RNA visualization at single-cell or single EV level, on the other hand, can provide additional spatial information enabling a better mechanistic understanding of RNA trafficking by EVs.

2.2. EV-RNA visualization

To spatially resolve EV-RNA and study its inter- and intracellular trafficking, the most straightforward strategy is RNA imaging after labeling exogenous RNA using chemical dyes and subsequent loading into EVs after their isolation. This method can be adopted to visualize EV uptake in target cells. For instance, it has been demonstrated with confocal microscopy that EVs (obtained through 0.22 μm filtration followed by ultracentrifugation at 120,000*g*) loaded with Alexa Fluor 488-labeled siRNA were taken up by monocytes and lymphocytes resulting in knockdown of the targeted mRNA expression [42]. This also confirms the hypothesis that EVs can be exploited to deliver exogenous RNA. An interesting application of labeling RNA with organic dyes is the analysis of the underlying mechanisms responsible for uptake. For example, one study demonstrated strong co-localization of Cy5-siRNA loaded EV mimics (obtained through extrusion of cells through a 1 μm membrane followed by Optiprep densitiy gradient ultracentrifugation at 100,000*g*) and markers of clathrin- and caveolae-mediated endocytosis shortly after EV addition to MCF-7 cells. On the other hand, co-localization with a macropinocytosis marker was limited. This suggests that mainly clathrin- and caveolae-mediated endocytosis are responsible for uptake of the EV-mimic in MCF-7 cells [43]. By following co-localization of siRNA with other markers of the endolysosomal pathway, the fate of siRNA in the recipient cell

may be studied over time. Nevertheless, RNA labeling with cell-impermeable dyes, such as Alexa Fluor and Cy5, cannot be applied for the visualization of endogenous RNAs, as it requires chemical conjugation of the RNA of interest. However, several membrane-permeable dyes exist that are selective for RNA and do not require conjugation, including E36 [44], Styryl-TO [45] and SYTO-RNAselect [46]. Only the latter has successfully been employed for the staining of endogenous EV-RNA and visualization of RNA intracellularly [46,47]. Nonetheless, SYTO-RNAselect and other membrane-permeable dyes are not suitable for imaging of specific transcripts and suffer from high background signals, potentially as a result of dye aggregation. To overcome these limitations, more specific RNA labeling strategies are required.

Molecular beacons (MBs) are DNA probes that have been designed to detect RNA molecules with high sequence specificity. MBs are attached to a fluorophore at one end and a fluorescence quenching molecule at the other end. MBs also contain a stem-loop that holds the fluorophore and quencher in close proximity to each other, resulting in quenching of fluorescence. Upon hybridization of the probe and target RNA, the MB undergoes a conformational change that increases the distance between fluorophore and quencher, resulting in the emission of light upon excitation (Fig. 1) [48]. This strategy has been used to visualize and quantify miRNA inside EVs. In these studies, introduction of miR-21-targeting MBs into EVs using streptolysin O (SLO), a bacterial endotoxin that reversibly creates pores in biological membranes, resulted in a higher signal compared to EV incubation with non-targeting MBs [49,50]. MBs have also been adopted for multiplexed detection of two distinct miRNAs and to demonstrate uptake of MB-containing EVs (obtained through Total Exosome Isolation™) in MCF7 cells [51]. An important consideration for quantification of RNA content with MBs, however, is the potential competition of these MBs with RNA-binding proteins. RNAs are often complexed with, for instance, Argonaute proteins or ALIX, which are key regulators of RNA loading in EVs [30]. As a consequence, potentially, not all RNA cargo can be hybridized with the delivered MBs. Besides the RNA levels in EVs, the amount of fluorescence is also dependent on the delivery efficiency of MBs in the EV lumen. Therefore, on a single EV level, employing MBs is not a reliable detection strategy, which limits its application to detecting RNA in a population of EVs. The potential of MBs to also obtain spatial EV-RNA information in live cells will be discussed further below.

To circumvent the issues in MB-based RNA imaging related to MB loading into EVs, studying genetically engineered RNA of EVs loaded before isolation is a promising alternative strategy. A well-established technique that has been used to visualize specific RNAs is derived from the bacteriophage MS2. The coat protein of bacteriophage MS2 (MCP) can recognize and bind specific stem-loop structures of (viral) RNA. Introduction of multiple copies of the stem-loop into an RNA of interest enables labeling of the RNA by multiple MCPs fused to a fluorescent protein (FP) (Fig. 2) [52]. For example, expression of the MCP-GFP fusion protein together with a reporter mRNA containing 24 MS2 binding sites (MBS) yields a punctate mRNA staining in the cytoplasm of living cells [53]. A major drawback of this method, however, is the high background signal that is caused by unbound MCP-GFP in the cytoplasm. This background is partly reduced by the fusion of a Nuclear Localization Signal (NLS) to MCP-GFP, ensuring that unbound MCP-GFP will be translocated into the nucleus. Even though the MS2 system is often used in live-cell mRNA imaging, it has been used in only one study to detect mRNA in an isolated pool of EVs. Here, Gli36 glioma cells were transfected with a plasmid encoding MCP-GFP-NLS and a reporter plasmid encoding PalmtdTomato mRNA containing multiple MBSs. After isolation of the EVs (obtained through 0.8 or 0.22 μm filtration followed by ultracentrifugation at 100,000*g*), co-localization of green and red fluorescence, originating from thePalmtdTomato transcript in the EV lumen and PalmtdTomato, a palmitoylated FP that labels the EV membrane, respectively, was demonstrated using confocal microscopy with a diffraction limit of approximately 200–300 nm [54]. This indicates that the PalmtdTomato mRNA was in or in close proximity to the isolated EVs. A drawback of MS2-based RNA visualization is the inability to detect unmodified endogenous RNA. The application of this system in real-time imaging will be further discussed below.

3. Fluorescence *in situ* hybridization

As discussed above, the techniques that have been applied to study EV-RNA lack sensitivity to image low abundance endogenous transcripts or have not been applied to spatially resolve EV-RNA [49,51,54]. As the number of transcripts per EV is very low [31], highly sensitive, preferably single-molecule, methods are required to visualize EV-RNA trafficking. In this chapter, the approaches will be discussed that have potential for the application in sensitive EV-RNA imaging in fixed cells or tissue. Table 1 gives an overview of these approaches.

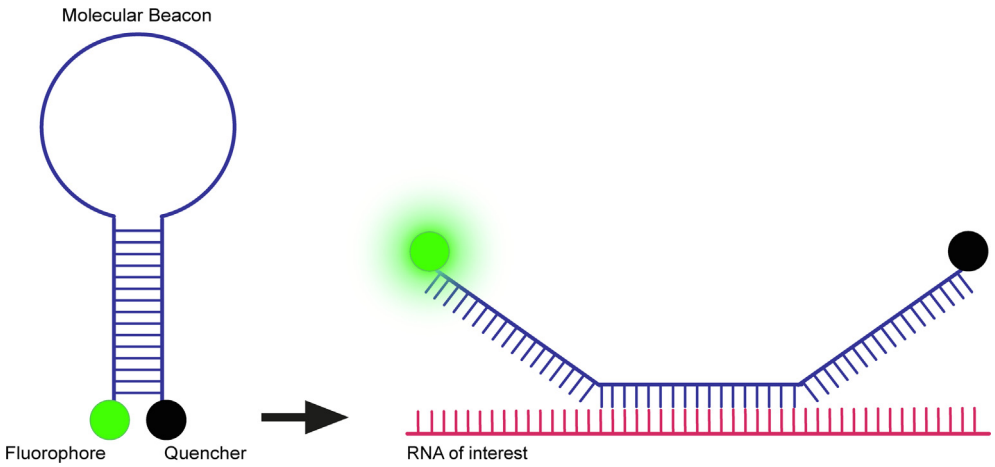

Fig. 1. Principle of RNA detection with molecular beacons. The MB is a DNA oligonucleotide that forms a hairpin structure, and contains a fluorophore at one end and a quencher at the other end. Upon intracellular/intraluminal delivery and hybridization of the MB with target RNA, the MB undergoes a conformation change that results in a fluorescent signal, as the quencher and fluorophore are separated.

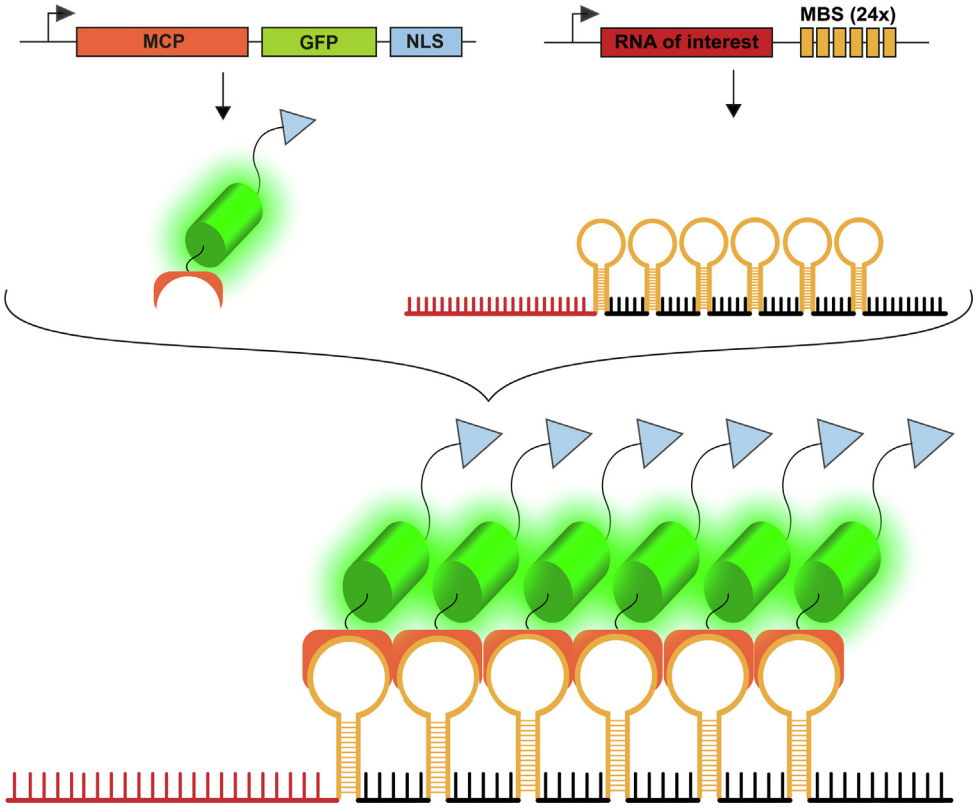

Fig. 2. Schematic representation of RNA imaging with the MS2 system. Plasmids encoding the MCP-GFP-NLS fusion protein and the exogenous target RNA with MBSs are transfected. After the expression of the protein and transcript, MCP can bind the MS2-binding sites enabling cytoplasmic GFP expression. When not bound, the fusion protein will be translocated into the nucleus.

Table 1
Overview of the various FISH approaches.

Technique	Advantages	Limitations	RNA type (long/small)	Study
smFISH	– Single-molecule visualization – High specificity	– Limited number of transcripts can be detected simultaneously – Not applicable for small RNAs	Long	[57,58]
bDNA amplification	– Single-molecule visualization (Long RNA only) – High specificity	– Limited number of transcripts can be detected simultaneously	Long and small	[61,67]
HCR	– Single-molecule visualization (Long RNA only)	– Limited number of transcripts can be detected simultaneously – Risk of high background signals	Long and small	[65,66]
Padlock probe and RCA	– Single-molecule visualization – High specificity	– Limited number of transcripts can be detected simultaneously	Long and small	[68,69]
FISSEQ	– Simultaneous detection of ~ 8.000 transcripts	– Limited sensitivity (~200 – 400 mRNA molecules) – Not (yet) suitable for single-cell profiling	Long	[72]
MERFISH or seqFISH	– Single-molecule visualization – Simultaneous detection of ~ 10.000 genes	– Not (yet) suitable for the detection of RNAs < 400-nt – Requires super-resolution or expansion microscopy	Long	[73–77]

3.1. Single-molecule fluorescence in situ hybridization

In situ hybridization (ISH) is a method developed to visualize specific nucleic acid sequences by hybridization with labeled probes in fixed cells or tissues. Fluorescence *in situ* hybridization (FISH) was proposed as a more sensitive and cheaper alternative to radiolabeled *in situ* hybridization (Fig. 3A). Hereby, covalent attachment of a fluorophore to a probe that can specifically recognize and hybridize a target DNA/RNA enables subcellular localization of specific nucleic acids using fluorescence microscopy [55]. FISH has been previously used to visualize RNA in EV donor and recipient cells *in vitro,* highlighting the ability to study intercellular RNA trafficking using this technique [56]. However, the detection of transcripts with conventional FISH is limited to highly abundant genes owing to the lack of specificity caused by off-target hybridization and the lack of sensitivity. Importantly, RNA labeling with only one fluorophore does not allow the differentiation between on– and off-target signal. Strategies to improve the signal-to-noise ratio (SNR) include the use of a few multiply labeled 50-nt probes [57] or a multitude of singly labeled 20-nt

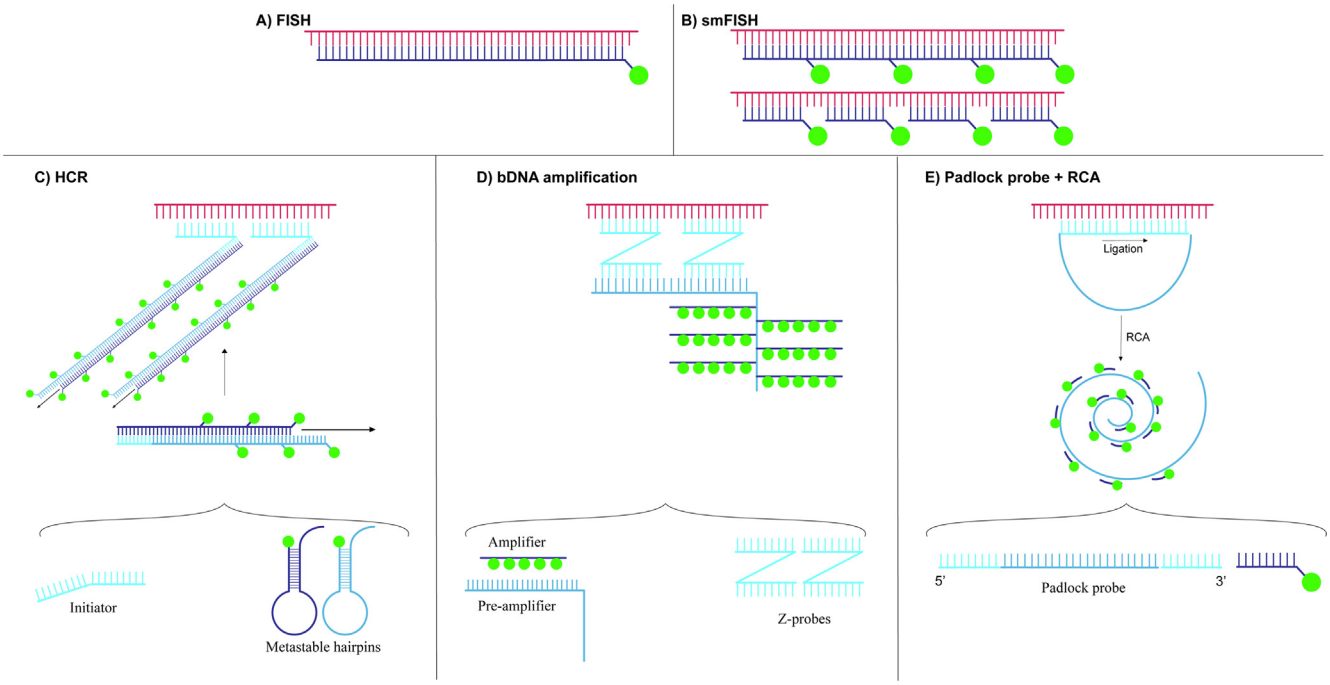

Fig. 3. Schematic overview of the various fluorescence *in situ* hybridization techniques. (A) Conventional RNA FISH. The target RNA (red) is recognized and hybridized by a specific DNA probe (blue) conjugated to a fluorophore (green). A fluorescent signal is emitted. (B) smFISH according to Femino et al. [57]– upper – and Raj et al [58] – lower. Hybridization of one probe containing multiple fluorophores or multiple probes containing a single fluorophore with the target RNA increases sensitivity compared to conventional FISH, enabling the detection of single RNA molecules *in situ*. (C) Hybridization chain reaction for signal amplification. An initiator oligonucleotide hybridizes the target RNA and a metastable hairpin attached to a fluorophore ensuring a conformational change and binding of a second hairpin with fluorophore. A chain reaction is initiated leading to fluorescence amplification. (D) bDNA amplification. Two Z-probes hybridize with the target RNA and a single preamplifier. Subsequently, the amplifier, which is conjugated to multiple fluorophores, binds the preamplifier and emits fluorescence, enabling single-molecule RNA detection with reduced background signal. (E) Padlock probe hybridization and RCA. A padlock probe containing two target-specific sequences at both ends hybridizes with the target RNA. Subsequent ligation of both ends linearized the padlock probe that can be amplified using RCA. Next, multiple fluorescent probes can bind the amplified padlock probe ensuring signal amplification. (For interpretation of the references to color in this figure legend, the reader is referred to the web version of this article.)

probes [58]. It has been demonstrated that with either approach, RNA imaging with single-molecule sensitivity can be obtained. Therefore, these approaches will be referred to as single-molecule FISH (smFISH), hereafter (Fig. 3B). The latter approach ensures the best sensitivity since potential self-quenching as a result of fluorophore interaction within probes is prevented. In addition, the fluorescent signal is less prone to variability with only one fluorophore attached to each probe [58]. Using smFISH, mRNA trafficking by tunneling nanotubes in co-culture has been visualized, indicating the potential of smFISH to also image mRNA trafficking by EVs *in situ* [59]. The detection of small RNAs by smFISH, however, is confounded by their size. For example, miRNAs are typically ~ 22-nt in length [60], whereas with smFISH as described by Raj *et al.* [58] multiple probes of each 20-nt are required. Therefore, this technique is limited to imaging of long RNA species such as mRNAs and long non-coding RNAs. Interestingly, smFISH is also compatible with immunohistochemistry or protein labeling [61]. This enables the study of intracellular trafficking of endogenous RNA through simultaneous imaging of, for instance, RNA, EVs and endocytic markers.

Interestingly, smFISH is also compatible with more complex 3D tissues, such as organoids or whole-mount embryonic organs [62,63]. This may allow studying of EV-RNA trafficking mechanisms in a biologically more relevant approach. Nonetheless, when applying any FISH technique, it is essential to preserve the precise biological structure when fixing the tissue. Importantly, tissue-fixation with formaldehyde is associated with EV loss, especially at higher temperatures by the reversible nature of formalin cross-links. Therefore, EV-RNA imaging with FISH may be challenging. A possible approach to overcome this includes a second fixation step that creates irreversible crosslinks between proteins, retaining EVs *in situ* [64].

3.2. Fluorescent signal amplification

To image small RNAs, which are predominantly present in EVs [28–30], with high sensitivity, RNA labeling with multiple fluorophores should be achieved in an alternative manner than conventional smFISH. Signal amplification of a single probe is a potential approach to facilitate this. Moreover, for longer RNA species signal amplification can enable imaging with, for example, simpler fluorescence microscopes using lower magnification objectives. Methods of fluorescence amplification include hybridization chain reaction (HCR), branched DNA amplification (bDNA) and rolling circle amplification (RCA). With HCR, sets of probes are hybridized to the target RNA. These probes contain an initiator sequence that can assemble to a metastable DNA hairpin structure, which is attached to a fluorophore. The DNA hairpin will undergo a spontaneous conformational change and is then able to bind a second metastable hairpin that is also attached to a fluorophore. This reaction will repeat itself, initiating a chain reaction [65] (Fig. 3C). Recently, the HCR method has been validated in a study demonstrating the simultaneous imaging of miRNA and mRNA in fixed retinal tissue [66]. Nonetheless, the main drawback of HCR is a lack of specificity caused by spontaneous amplification without proper initiation, which can result in higher background signals.

bDNA amplification is an alternative and more specific approach that uses multiple target-specific, 20nt Z-shaped DNA probes. The upper regions of two independent Z-probes can be specifically hybridized to a single preamplifier. Subsequently, the

amplifiers containing many fluorophores can be bound to the preamplifiers at multiple binding sites. In such a way, bDNA amplification increases the fluorescence per DNA probe (Fig. 3D). This unique Z-probe/preamplifier hybridization strategy also establishes a higher specificity compared to HCR, as off-target RNA binding of only one probe will not induce signal amplification. Using this approach, multiplexed *in situ* imaging of up to four separate mRNAs at the single-molecule level has been demonstrated [67]. For the amplification and detection of single small RNAs, however, bDNA amplification has not yet been adopted. As it is challenging to distinguish between fluorescent signals derived from bound and unbound (pre)amplifiers, HCR and bDNA amplification have the most potential for single-molecule detection of (small) RNA species that can be bound by multiple initiators or Z-probe pairs. Therefore, to obtain a sufficient SNR for single-molecule detection, these signal amplification strategies may be limited to the detection of EV-RNAs > 80nt.

Last of all, padlock probe hybridization followed by RCA is a promising signal amplification strategy that has been successfully used to spatially resolve individual miRNAs. Padlock probes are DNA probes containing a target-specific sequence at the 5′ and 3′ end and a non-specific sequence between each end. Hybridization to the RNA of interest and subsequent ligation of both ends of the padlock probe effectively circularizes this probe [68,69]. The circular probe is subsequently amplified with RCA using the miRNA as a primer. Next, the amplified DNA containing multiple copies of the target miRNA can be hybridized by multiple fluorescently labeled probes [69] (Fig. 3E). Since the miRNA in this approach serves as the ligation template for the padlock probe and as a primer for RCA, this method ensures high sensitivity and specificity.

3.3. Transcriptome-scale RNA detection in situ

To visualize the complete transcriptome of specific EV populations, multiplexed imaging of thousands of RNA species is required. Multiple groups have worked on imaging multiple mRNA species simultaneously with smFISH, however, the maximum number of detectable RNA species in one experiment remains limited to ~ 30 [70,71]. One technique that was developed to enable multiplexed imaging is fluorescence *in situ* sequencing (FISSEQ). It relies on *in situ* reverse transcription of RNA molecules into short cDNA fragments, a process that is primed by random hexamers. These fragments are subsequently circularized and amplified in multiple cycles followed by hybridization of a unique sequencing primer and fluorescent probe ligation to the primer. After fluorescence imaging, the fluorophore is cleaved, and fluorescent probe ligation is repeated every fifth base pair. Afterwards, the complete sequencing process is repeated with four additional unique sequencing primers to enable the sequencing of all intermediate bases. As the sensitivity of FISSEQ is dependent on the process of reverse transcription, the estimated lower detection limit is currently ~ 200–400 mRNA molecules, hence this method is not suitable for low abundance RNAs [72].

Multiplexed error robust FISH (MERFISH) or sequential FISH (seqFISH) is a strategy that significantly enhances the number of RNA species that can be detected in a single FISH experiment. This approach is more sensitive than FISSEQ. In MERFISH, fixed cells are treated with unique encoding probes that act as a scaffold between the target RNA and a secondary readout probe. These encoding probes consist of an mRNA targeting sequence to facilitate *in situ* hybridization and two flanking read-out sequences for secondary probe hybridization. To increase the SNR, each RNA molecule is labeled with multiple encoding probes. The encoding probes each contain a unique combination of the N readout sequences. Successive N hybridization rounds with the N unique read-out probes yields a positive signal (1) or negative signal (0) for each round. In this manner, transcript-specific binary codes can be written (Fig. 4). For N readout probes or hybridization rounds, $2^N - 1$ different RNA species can be imaged, meaning that the number of RNA species that can be imaged increases exponentially with the number of hybridization rounds. As proof-of-concept, 1001 RNA species have been quantified and spatially-resolved in a single experiment [73,74]. Combining MERFISH with branched DNA amplification has allowed signal improvement while using fewer encoding probes, however, this strategy only remains suited for imaging of longer RNA species (>480-nt) [75]. Now, MERFISH has been used to reveal the subcellular RNA localization of ~ 10.000 transcripts, indicating the enormous potential to quantify and image RNA transcriptome-wide [76]. SeqFISH is a similar approach. Here, however, barcoding is performed directly with multiple hybridization rounds of a set of smFISH probes attached to fluorophores with distinct colors in each round [77]. MERFISH or seqFISH in combination with EV labeling has the potential to visualize EV-RNA content and their subcellular localization, and for instance, to make a comparison between RNA-cargo of subpopulations of EVs. Although promising, to spatially-resolve each transcript-specific signal with microscopy, super-resolution is required. Therefore, this barcoding approach is a less accessible technique. To overcome this issue, MERFISH has been combined with expansion microscopy [78]. In addition, seqFISH + has been developed where the color palette, and therefore the number of images, is increased significantly. By recombining all separate images in a similar manner as in single-molecule localization microscopy (SMLM), a super-resolution image can be reconstructed using a conventional confocal microscope [79]. A second issue is that, as the degree of multiplexing increases, off-target binding of FISH probes may increase background signals. To address this issue, split-FISH was developed. Hereby, an additional encoding probe pair is included, which is delivered as split probe. It is designed to bind the conventional encoding probes only when both split probes are hybridized to the RNA [80]. This decreases the risk of off-target encoding probe binding. Therefore, this design may increase the accuracy of RNA profiling.

4. Live-cell RNA tracking

The previously discussed FISH techniques are not applicable for live-cell imaging, mainly as it requires cell and EV permeabilization and subsequent washing steps to remove the unbound probes. Real-time EV-RNA tracking would enable studying the dynamic process of cargo sorting, intercellular trafficking, and RNA transfer. As discussed before, MBs and MS2-systems have only been used for imaging RNAs in an isolated pool of EVs [49,54]. Their potential as imaging techniques for live-cell EV-RNA tracking will be highlighted in this chapter. Moreover, the application of CRISPR/Cas technology and fluorogenic RNA aptamers for RNA imaging will be discussed. Table 2 gives an overview of all discussed methods in this chapter.

4.1. Molecular beacons

Upon intracellular delivery of MBs and hybridization with the (endogenous) target RNA, segregation of fluorophore and quencher results in the emission of a specific RNA signal. In this manner, individual RNA molecules can be dynamically tracked in living cells [81,82]. For example, following intracellular MB delivery, several studies have investigated the mechanisms underlying intracellular trafficking of endogenous mRNA or pre-miRNA in real-time in mammalian axons and revealed their subcellular localization [83,84]. However, a major concern with this strategy is that the cytosolic delivery of MBs by methods that require membrane pore

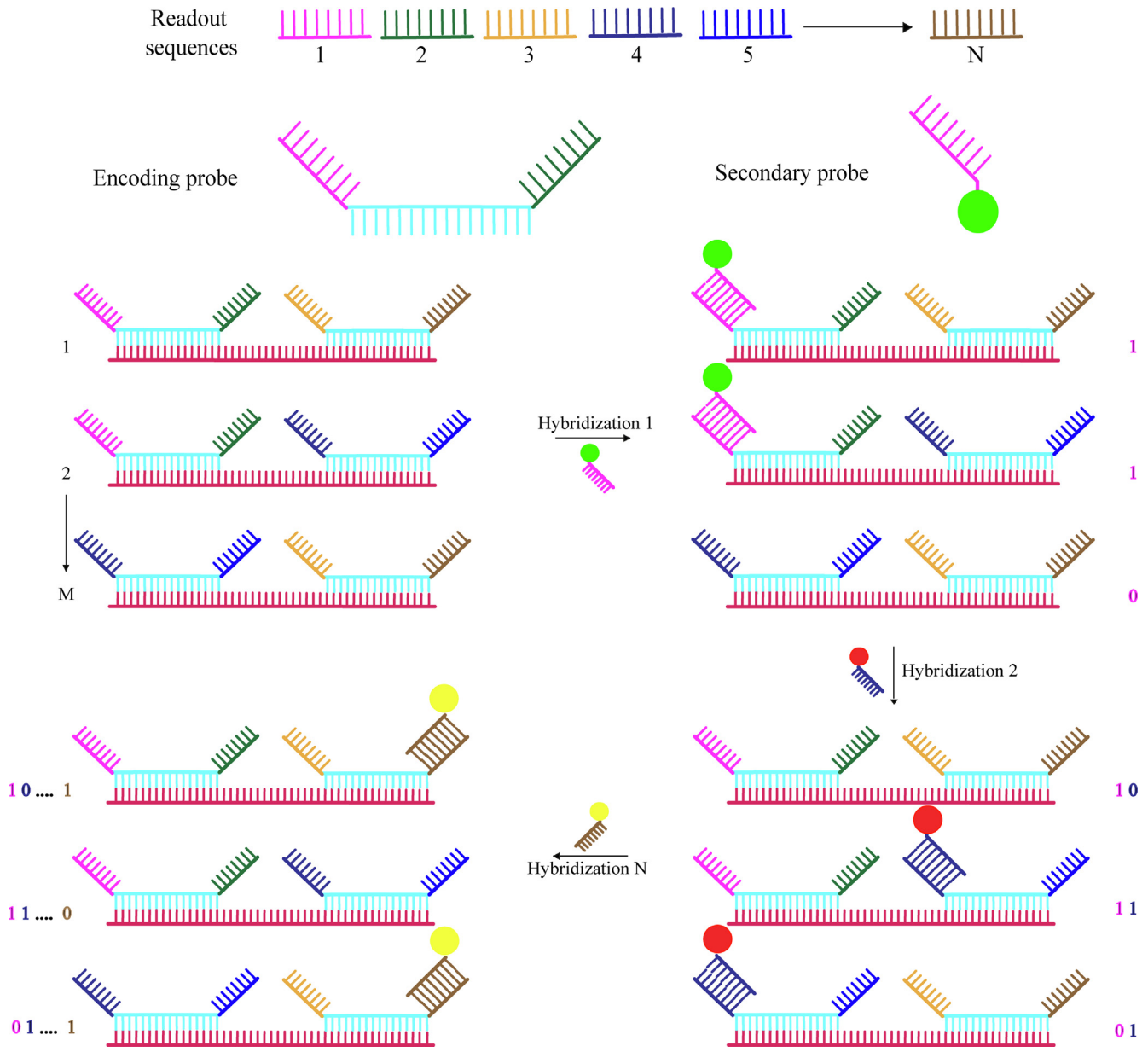

Fig. 4. Graphical representation of the MERFISH method. M transcripts are hybridized with 192 encoding probes containing N unique readout sequences in total. The encoding probes will be hybridized subsequent rounds with N unique secondary probes each complementary to one of the readout sequences. Each hybridization round will give a positive (1) or negative (0) signal for the genes, thereby writing a transcript-specific binary code. Between each round photobleaching is applied. The total number of transcripts that can be identified, both spatially and qualitatively, equals $M = 2^N - 1$.

formation, such as electroporation or SLO, can induce cell damage. One study reports live cell tracking of MB-miRNA trafficking by EVs (obtained through ExoQuick-TC Precipitation) using SMLM. However, as no strategy was applied to load the MB inside the vesicles, it is unlikely that miRNA in the vesicle lumen is observed here [85]. Moreover, it is unexplored if MBs associated with RNAs can be endogenously loaded in EVs to study RNA trafficking in real-time or that MBs are only suitable for free RNA labeling in donor and recipient cells. Recently, it has been demonstrated that miR-495-specific MBs complexed with the cell-penetrating peptide TAT enables imaging of miRNA-495 in red blood cell-derived EVs (obtained through size exclusion chromatography using a qEV column). Moreover, MB-miRNA-495-TAT could be internalized in live red blood cells [86]. These findings both support the potential of studying EV-RNA trafficking with MBs. Importantly, for single-molecule detection of small RNA species MBs cannot be used. On the other hand, for mRNAs and lncRNAs single-molecule sensitivity can be obtained by employing MBs that target multiple sites on an individual transcript, as seen for smFISH [83].

4.2. RNA-binding fluorescent proteins

As mentioned above, the bacteriophage MS2 system holds potential for live-cell RNA imaging [53]. This approach has been previously used to image mRNA in EVs that were loaded before isolation [54], therefore, this strategy is feasible to load the target RNA complexed with MCP-GFP into EVs. Moreover, MS2-derived systems have been previously used to show, for instance, intracellular RNA sorting into subcellular locations in live neuronal cells [87]. Hence, this system may be applied to obtain insight into RNA sorting mechanisms and inter- and intracellular trafficking of EV-RNA in real-time. Nonetheless, unbound MCP-FP causes high back-

Table 2
Overview of the techniques suited for live-cell RNA tracking.

Technique		Advantages	Limitations	RNA type (long/small)	Study
Molecular Beacons		– Single-molecule sensitivity – Imaging of endogenous unmodified RNA	– Requires toxic intracellular delivery agents – Possibly competes with endogenous RNA binding proteins for target binding	Long	[83,84]
RNA-binding fluorescent proteins	MS2-derived systems	– Single-molecule sensitivity	– Background from unbound FPs – Requires RNA modification	Long	[87,88]
	Pepper	– Single-molecule sensitivity – Low background signals	– Requires RNA modification	Long	[89]
CRISPR/Cas		– Imaging of endogenous unmodified RNA – High labeling efficiency	– Background from unbound FPs – Not suitable for low abundance transcripts – Possibly competes with endogenous RNA binding proteins for target binding	Long	[92,97]
Fluorogenic RNA aptamers	Conventional RNA aptamers	– Single-molecule sensitivity (long RNA only) – Low background signals	– Requires RNA modification	Long and small	[98–104]
	AiFC	– Low background signals – Imaging of endogenous unmodified RNA	– Restricted to long RNAs – Restricted to high abundance transcripts – Possibly competes with endogenous RNA binding proteins for target binding	Long	[108]
	CHARGE	– Single-molecule sensitivity – Imaging of endogenous unmodified RNA	– Does not provide spatial information – Possibly competes with endogenous RNA binding proteins for target binding	Small	[109]

ground fluorescence. Besides the incorporation of an NLS, splitting the FP into two non-fluorescent proteins to increase specificity can circumvent this issue. In this approach, the MS2 system is combined with the analogous PP7 system. Both MCP and PCP are expressed as a fusion protein with a partial FP and bind a 12x-MS2-PP7 tandem binding site array in the reporter mRNA. Only when MCP and PCP are both bound to their specific stem-loops a fluorescent signal can be observed [88]. Self-association of the FP may occur at high concentrations, which must be taken into consideration. Another novel strategy to increase the SNR employs fluorogenic proteins. These conditional FPs are attached to a peptide that promotes protein degradation unless stabilized by the specific Pepper RNA motif. Similar to the MS2 system, incorporation of multiple copies of Pepper into the mRNA of interest enables single-molecule detection using fluorescence microscopy [89]. Unbound FP will be degraded in this approach, which prevents high background signals and therefore improves the SNR.

4.3. CRISPR/Cas-based RNA detection

CRISPR/Cas9 is a bacterial derived adaptive immune system that is being intensively researched for its gene editing capabilities. It comprises the CRISPR associated endonuclease 9 (Cas9) that complexes with a specific single-guide RNA (sgRNA). The Cas9/sgRNA complex can recognize a specific sequence in the DNA, the protospacer adjacent motif (PAM), and subsequently bind and digest the target DNA upstream in the gene [90]. The intrinsic ability of Cas9/sgRNA to form specific RNA-DNA hybrids can be exploited for RNA imaging. By providing a PAMmer, which is a small DNA/RNA modified oligonucleotide containing the Cas-specific PAM sequence, a catalytically inactive Cas9 (dCas9)/sgRNA complex is able to bind a ssRNA target with high affinity (Fig. 5). Furthermore, 2′OMe modification of the PAMmer prevents degradation by RNase H [91]. This strategy has been successfully employed for live-cell mRNA-imaging using a dCas9-GFP fusion protein. Nonetheless, this system has only been applied for imaging highly abundant mRNA and is not sufficient for tracking of less abundant RNA species or for single-molecule detection [92]. To increase sensitivity, targeting multiple sites per mRNA or lncRNA with dCas9 may be an option. An important consideration for this, however, is the possible competition with endogenous RNA binding proteins. A second strategy to increase sensitivity is to increase the fluorescence associated with Cas9, for example through the SunTag system [93,94]. On the other hand, the fluorescent signal of off-target hybridization and unbound Cas9 also increases, which may decrease the SNR.

More recently, it has been shown that RNA targeting with dCas13, a CRISPR effector with intrinsic RNA-targeting capabilities, enables RNA visualization without co-transfection of a PAMmer [95]. Similarly, it has been demonstrated that the *Streptococcus aureus* Cas9 (SaCas9) is able to target RNA without requiring a PAMmer in contrast to SpCas9, the most commonly used Cas9 homolog [96]. RNA imaging with catalytically inactive Cas13-FP or SaCas9-FP fusion proteins may be more efficient, as RNA targeting is independent of the PAMmer. For Cas13, several homologs have been fused with GFP and screened for their ability to target the medium abundance (50–60 copies) lncRNA NEAT1 in HeLa cells disclosing the dPspCas13b homolog to be highly efficient for real-time PAMmer-independent lncRNA localization. A direct comparison in RNA visualization revealed that the mean SNR per fluorescent spot for Cas13-based imaging is twice as low as reported for the MS2 system [97].

The main advantage of the CRISPR/Cas technology for RNA labeling is that it does not require complicated genetic manipulations. It has been successfully employed to track endogenous RNAs in live cells, however not with single-molecule sensitivity. In addition, due to the high molecular weight of the FP-labeled CRISPR/Cas, it may be possible that RNA imaging following this approach alters the RNA functionality. Interestingly, Cy3-labeling of the sgRNA instead of GFP labeling of the dPspCas13b was also successful in real-time RNA tracking and might be interfering less with EV-RNA trafficking [97]. Moreover, due to the large size of Cas9/Cas13 it is unlikely that this method can be efficiently used for the imaging of endogenously loaded RNAs inside EVs. Therefore, this application may be limited to the imaging of free high abundance RNAs in donor or recipient cells enabling the study of, for instance, subcellular endogenous RNA locations in real-time.

4.4. Fluorogenic RNA aptamers

The previously discussed techniques that have potential for live-cell EV-RNA imaging all require the introduction of cell-impermeable probes or FPs. Unlike proteins, no RNAs with intrinsic fluorescent capabilities are known. Efforts to approximate FPs with RNA sequences initiated with the discovery of a small molecule, 3,5-dimethoxy-4-hydroxybenzylidene imidazolinone (DMHBI)

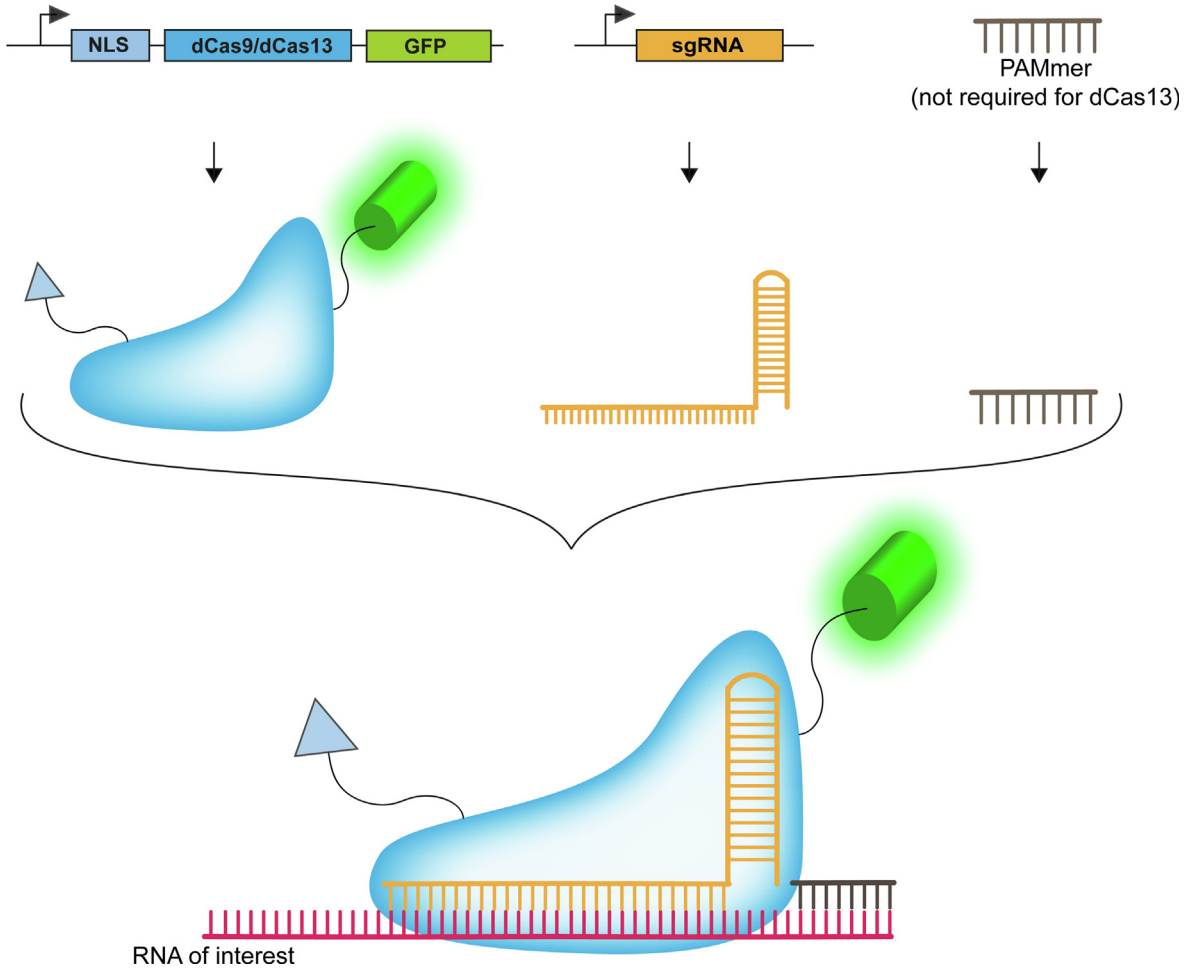

Fig. 5. The CRISPR/Cas system for live-cell RNA tracking. Cells are transfected with (1) a plasmid encoding the catalytically inactive dCas9/dCas13 protein fused to an NLS sequence and GFP (2) a plasmid encoding the sgRNA specific for the target RNA sequence and (3) a PAMmer, which is an RNase resistant oligonucleotide, enabling target site recognition of the dCas9/sgRNA complex. RNA targeting with dCas13 does not require the transfection of the PAMmer. Unbound NLS-dCas9/dCas13-GFP will be directed to the nucleus.

that resembles the structure of the activated fluorescent complex, HBI, in GFP but does not have fluorescent activity itself. Such small non-fluorescent molecules that have conditional fluorescent properties are called fluorogens. Screening of a library of RNA molecules for their ability to bind DMHBI and activate fluorescence resulted in the discovery of the first fluorogenic RNA aptamer called Spinach. Introduction of the 96-nt Spinach sequence into a target RNA facilitates the detection of these RNAs in live cells after incubation with the cell-permeable DMHBI (Fig. 6A) [98]. Later, optimization of the screening protocol focusing on the cellular performance of the aptamers resulted in the discovery of the enhanced aptamer Broccoli. It has increased thermostability and expression levels in HEK293T cells compared to Spinach. Moreover, Broccoli is composed of only 49-nt simplifying incorporation of the aptamer in the target RNA sequences without disrupting their functions [99]. Since then, multiple enhanced RNA aptamers have been identified or developed binding various fluorogens. The most promising aptamers including RNA Mango [100], Pepper (different than the RNA binding motif) [101], O-coral [102] and Riboglow [103] all comprise fewer nucleotides or report higher sensitivity and specificity in live-cell RNA imaging in comparison with the conventional aptamers. A recent study demonstrates that following mRNA labeling with 24 RNA mango arrays compared to 24 MS2 stem-loop sequences, a significantly higher SNR is observed [104]. Importantly, it is also the first study in which single-molecule detection of mRNA has been demonstrated using fluorogenic aptamers. Interestingly, incorporation of fluorogenic aptamer sequences in the sgRNA stem-loops has also been proposed as indirect labeling strategy for CRISPR/Cas-based imaging of endogenous nucleic acids without requiring a FP tag [101,105]. By the cell-permeable nature of the fluorogens, straightforward labeling and live-cell visualization of RNA molecules intracellularly are facilitated. It is plausible, yet unproven, that these molecules can also penetrate into subcellular compartments and into EVs, thereby enabling EV-RNA tracking. Following direct RNA labeling with conventional fluorogenic aptamers, however, it is not possible to image endogenous transcripts.

In parallel with the discovery of more sensitive aptamers, sophisticated methods have been developed for more specific and sensitive RNA imaging in live cells. For example, Spinach and Broccoli split-aptamers have been designed, whereby the original aptamer sequence is segregated into two partial sequences. These can be separately incorporated into target oligonucleotide sequences. Upon hybridization of both constructs, the split-aptamer reassembles into the active Spinach or Broccoli conformation, thereby enabling visualization of specific DNA/RNA-RNA hybridization events [106,107]. This principle is the fundament of the aptamer-initiated fluorescence complementation (AiFC) system (Fig. 6B). With AiFC, split-aptamers are incorporated into two RNA sequences. Both are complementary to specific sequences in

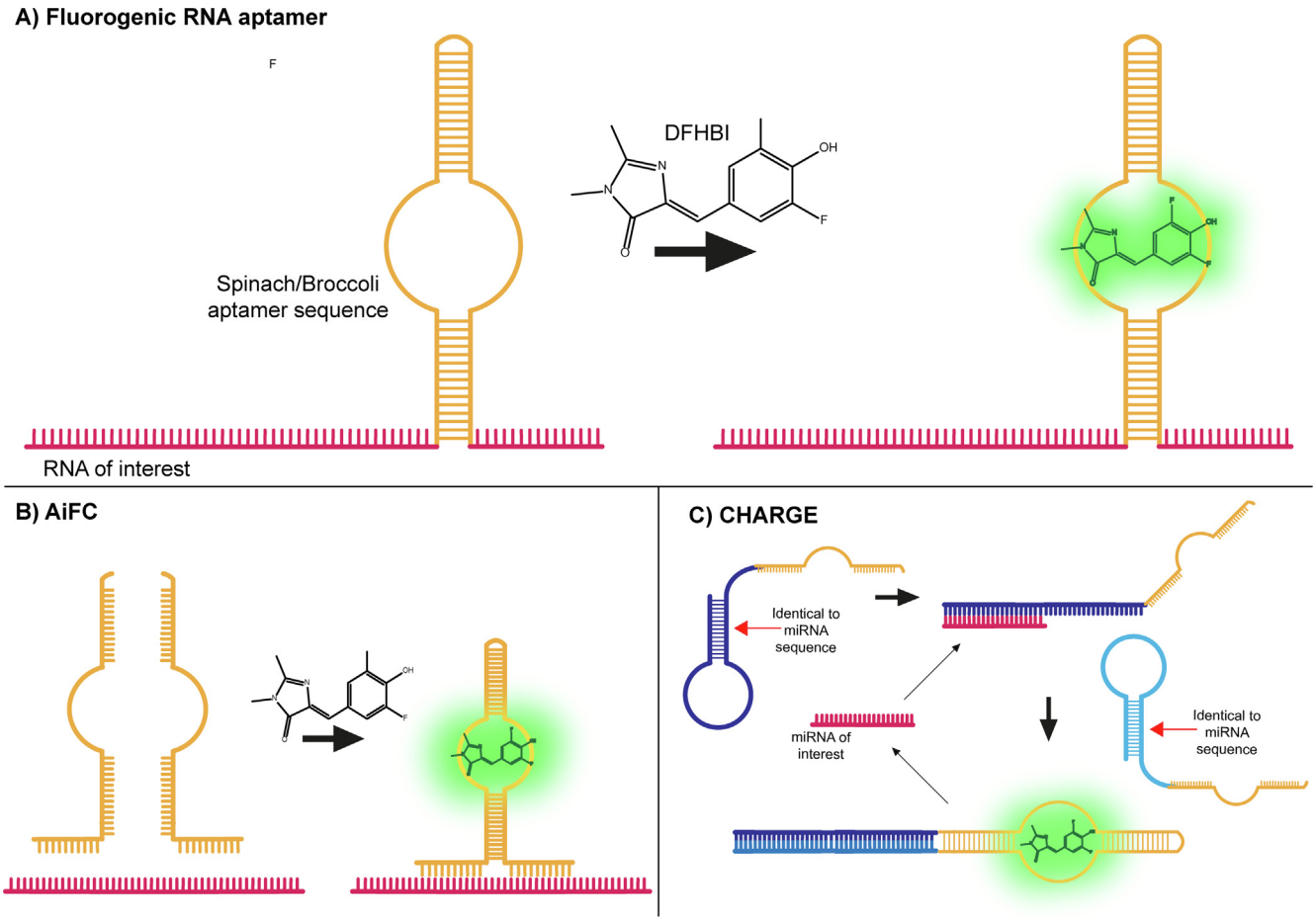

Fig. 6. Schematic overview of the various methods utilizing fluorogenic RNA aptamers for RNA visualization. (A) Principle of fluorogenic RNA aptamers for live-cell RNA imaging. The Spinach or Broccoli aptamer sequence is cloned into the target RNA. Cells expressing this transcript are treated with the non-toxic DFHBI, which can be captured into the RNA aptamer structure. DFHBI motion is limited when bound to the RNA aptamer resulting in energy release through light emission. (B) AiFC split aptamer method. Two RNA split-aptamer sequences contain a complementary sequence to the target RNA. When these hybridize with the target RNA, the split-aptamers are bound together forming the functional RNA aptamer. (C) CHARGE principle to increase the sensitivity of the RNA aptamer. Two hairpin structures, both containing the miRNA target sequence (red arrows), are hybridized to their complementary strand forming the stem-loop structure. They are attached to a split-aptamer sequence. The target RNA functions as a catalyst when hybridizing with the first hairpin. Subsequently, the second hairpin hybridizes with the first hairpin and finalizes the RNA aptamer sequence. Hereby, the target RNA is recycled. (For interpretation of the references to color in this figure legend, the reader is referred to the web version of this article.)

an individual target RNA. Transfection with plasmids encoding the split constructs enabled the visualization of endogenous β-actin mRNA in living cells, whereas neglectable signals were observed for cells that had been transfected with only one or neither of the split plasmids [108]. Visualization of smaller RNAs, however, poses a larger challenge. To facilitate this, a promising method, which resembles the fluorescent amplification by HCR as discussed for FISH, has been developed that increases the sensitivity. With this approach, the split-aptamer sequence is incorporated into two separate hairpin structures. Initially, the hybridization of both hairpins to the target sequence and to each other is hindered, as the complementary sequences are embedded in their stem. Only a specific target RNA can hybridize and open up one of the hairpins, allowing the assembly of both hairpins and, thereby, the full aptamer sequence. Finally, the target sequence is recycled. Therefore, this technique is named Catalytic Hairpin assembly RNA circuit (CHARGE) (Fig. 6C). It has been successfully used to image miR21 inside live bacterial cells with split-Broccoli, however, it still needs to prove feasibility in mammalian cells [109]. As the target RNA functions as the catalyst in this system, theoretically, high- and low abundance RNAs could be imaged with similar sensitivity. As the activated fluorophore is not bound to the RNA, however, no spatial information is provided.

5. Studying functional EV-RNA transfer

Following the labeling approaches described above for direct RNA visualization, EV-RNA loading and trafficking can be imaged. To demonstrate, however, that RNA cargo has escaped endolysosomal degradation and has been functionally delivered by EVs into the cytosol, detecting subcellular localization of RNA is not sufficient. When developing EV-based systems for therapeutic RNA delivery, accurately studying the mechanisms underlying functional delivery into recipient cells and the processes facilitating this is pivotal. Initially, the detection of functional transfer of RNA by EVs was mainly limited to measuring the biological effect of the transferred RNA in the recipient cells upon incubation with an isolated, concentrated pool of EVs that were loaded after isolation. For instance, the functional delivery of siRNA can be assessed by measuring the reduced expression levels of target mRNA using RT-qPCR or ddPCR, or gene knockout can be measured upon delivery of isolated EVs containing Cas9 mRNA and sgRNA [20]. Additionally, functional mRNA delivery in recipient cells can be assessed upon treatment with the protein translation inhibitor cycloheximide as control [54]. However, to closely resemble and study the natural transfer of endogenous RNAs by EVs *in vitro* it is essential to measure the effect of the RNA in co-culture of EV

donor and recipient cells rather than to treat cells with an isolated, and concentrated pool of EVs. Moreover, considering the limited number of RNA molecules per vesicle and low read-out sensitivity of these knockout/knockdown assays, they are not sufficient to measure the effects of functionally transferred endogenously loaded RNAs.

To investigate functional EV-RNA transfer in an experimental set-up that better simulates endogenous RNA trafficking, a reporter system has been developed employing Cre-loxP recombinase. The system requires two engineered cell lines: one donor cell line stably expressing a FP to distinguish donor cells from reporter cells and Cre, and a recipient cell line stably expressing a different FP followed by a stop codon and flanked by two lox P sites. Another FP gene is encoded in the plasmid downstream of the stop codon and is therefore not expressed. Delivery of Cre-mRNA followed by Cre protein expression in the recipient cells will result in the removal of the first FP gene and stop codon by recombinase. As a consequence, the second FP will be expressed resulting in a color shift in the recipient cells [110]. The Cre-loxP reporter system has been successfully used to show EV-mediated mRNA transfer *in vitro* [111] and *in vivo* [112,113]. Considering the small number of mRNA molecules loaded in EVs, these results suggest highly efficient functional transfer of RNA. Together with an increasing number of studies reporting EVs as key regulators in (patho)physiological processes, this underlines the therapeutical and biological importance of studying the mechanisms underlying this effective RNA delivery using the Cre-loxP system. The main drawback of the Cre-loxP reporter is that transfer of Cre protein, expressed in the EV donor cells, cannot be differentiated from functional Cre mRNA transfer. Another possible approach to detect functional mRNA delivery relies on the detection of translation in the EV recipient cell using SunTag mRNAs. Here, genetic engineering of 24 SunTag peptide sequences into the transcript of interest enables imaging of the nascent chain with single-molecule sensitivity. The SunTag sequences are specifically recognized by FP-coupled single-chain antibodies that can be expressed in the EV acceptor cells [114]. Similar to Cre-loxP, this approach may be affected by potential protein transfer by EVs. In contrast, theoretically, the functional transfer of any mRNA of interest can be assessed.

The above-described reporter systems are limited to the detection of large mRNA (or protein), thereby not allowing to detect functional transfer of small RNAs. Trafficking of these small RNAs may be distinct from that of intact mRNA in terms of loading and transfer efficiency. As mentioned above, EVs contain mainly small RNAs or fragmented mRNAs [28]. This underlines the need for an additional system that may be biologically more relevant to study the mechanisms involved in EV-mediated transfer of small non-coding RNAs in specific. To address this need, recently, a novel fluorescent reporter system has been developed, which allows the specific detection of functional sgRNA transfer *in vitro*. The CRISPR Operated Stoplight System for Functional Intercellular RNA Exchange (CROSS-FIRE) relies on a reporter cell line that stably expresses mCherry, a linker sequence with a sgRNA-specific target for CRISPR/Cas9, and two eGFP sequences, 1 or 2 nucleotides out-of-frame, respectively. Following the functional delivery of sgRNA into the recipient cell, a double-strand break will be induced by functional CRISPR/Cas9 resulting in a frameshift, causing eGFP to be permanently expressed in addition to mCherry [115]. The main advantages of CROSS-FIRE are the high sensitivity and the ability to simply detect functional transfer of sgRNA at a single-cell resolution using fluorescence microscopy and flow cytometry. Now, using Cre-LoxP and CROSS-FIRE, the functional delivery of both long and small RNAs can be measured with high sensitivity. This allows, for instance, the screening of proteins and genes involved in EV-mediated functional transfer of RNAs.

6. Conclusion and future perspective

EVs are a promising tool for the therapeutic delivery of RNAs, as they have the intrinsic ability to functionally transfer RNAs and may be less immunogenic compared to synthetic nanocarriers. Nonetheless, how EVs functionally traffic specific RNA molecules into target cells remains largely to be elucidated. Studying inter- and intracellular tracking of EV-RNA could increase our understanding of the biology underlying the functional delivery of specific RNAs by EVs. This review discussed the methods that are currently available to quantify and visualize EV-RNA. Additionally, it highlighted the available methods to assess functional transfer as well as novel approaches that can potentially be employed for these purposes.

The FISH techniques discussed here have the advantage that labeling is relatively straight forward. Using smFISH, single-molecule sensitivity can be obtained for *in situ* visualization of long RNA species. Moreover, signal amplification strategies may potentially be employed to image small EV-RNA species with single-molecule sensitivity. Live-cell imaging approaches require more complex labeling with overall lower sensitivity and specificity. However, they have the great advantage that they can be employed to visualize the dynamics of RNA loading, trafficking and transfer. The optimal choice to detect RNA depends on the type of transcript to be imaged, the required sensitivity and selectivity, and the number of RNA species to be imaged simultaneously.

Besides the progression in sophisticated labeling approaches, further advances in fluorescent microscopy may help to increase the overall detection sensitivity and resolution. For instance, a combination of both sensitive RNA labeling techniques and high-resolution microscopy could lead to optimal spatially resolved imaging. This is demonstrated for instance using sRNA-PAINT, whereby super-resolution compatible smFISH probes are successfully employed [116] or in a recent study that enables the imaging of specific RNAs with single-molecule sensitivity and nanoscale resolution by combining HCR amplification with expansion microscopy [117].

With the Cre-loxP and CROSS-FIRE reporter systems, we now have the tools to study the functional transfer of long and small RNA with single-cell sensitivity. As the techniques to fluorescently label and to detect RNA improve, employing them to image EV-RNA has the potential to elucidate the selective mechanisms that determine functional delivery. This includes the loading of specific transcripts and generation of functional subpopulations as well as intercellular trafficking, uptake and escaping lysosomal degradation. This will greatly contribute to the development of enhanced EV-based or EV-inspired systems for the functional delivery of therapeutic RNAs.

Declaration of Competing Interest

The authors declare the following financial interests/personal relationships which may be considered as potential competing interests: [P.V. serves on the scientific advisory board of Evox Therapeutics].

Acknowledgments

This work is supported by the European Research Council (ERC) Starting grant OBSERVE (# 851936) to P.V.

References

[1] S. Bajan, G. Hutvagner, RNA-based therapeutics: from antisense oligonucleotides to miRNAs, Cells. 9 (2020) 137, https://doi.org/10.3390/cells9010137.

[2] J.C. Kaczmarek, P.S. Kowalski, D.G. Anderson, Advances in the delivery of RNA therapeutics: From concept to clinical reality, Genome Med. 9 (2017), https://doi.org/10.1186/s13073-017-0450-0.
[3] S.F. Dowdy, Overcoming cellular barriers for RNA therapeutics, Nat. Biotechnol. 35 (2017) 222–229, https://doi.org/10.1038/nbt.3802.
[4] V.K. Udhayakumar, A. De Beuckelaer, J. McCaffrey, C.M. McCrudden, J.L. Kirschman, D. Vanover, L. Van Hoecke, K. Roose, K. Deswarte, B.G. De Geest, S. Lienenklaus, P.J. Santangelo, J. Grooten, H.O. McCarthy, S. De Koker, Arginine-rich peptide-based mRNA nanocomplexes efficiently instigate cytotoxic T cell immunity dependent on the amphipathic organization of the peptide, Adv. Healthc. Mater. 6 (2017) 1601412, https://doi.org/10.1002/adhm.201601412.
[5] Q. Chen, R. Qi, X. Chen, X. Yang, S. Wu, H. Xiao, W. Dong, A Targeted and stable polymeric nanoformulation enhances systemic delivery of mRNA to tumors, Mol. Ther. 25 (2017) 92–101, https://doi.org/10.1016/j.ymthe.2016.10.006.
[6] M.A. Oberli, A.M. Reichmuth, J.R. Dorkin, M.J. Mitchell, O.S. Fenton, A. Jaklenec, D.G. Anderson, R. Langer, D. Blankschtein, Lipid nanoparticle assisted mRNA delivery for potent cancer immunotherapy, Nano Lett. 17 (2017) 1326–1335, https://doi.org/10.1021/acs.nanolett.6b03329.
[7] H.Y. Xue, S. Liu, H.L. Wong, Nanotoxicity: A key obstacle to clinical translation of sirna-based nanomedicine, Nanomedicine. 9 (2014) 295–312, https://doi.org/10.2217/nnm.13.204.
[8] H. Lv, S. Zhang, B. Wang, S. Cui, J. Yan, Toxicity of cationic lipids and cationic polymers in gene delivery, J. Control. Release. 114 (2006) 100–109, https://doi.org/10.1016/j.jconrel.2006.04.014.
[9] L. Jiang, P. Vader, R.M. Schiffelers, Extracellular vesicles for nucleic acid delivery: Progress and prospects for safe RNA-based gene therapy, Gene Ther. 24 (2017) 157–166, https://doi.org/10.1038/gt.2017.8.
[10] O.M. Elsharkasy, J.Z. Nordin, D.W. Hagey, O.G. de Jong, R.M. Schiffelers, S.E.L. Andaloussi, P. Vader, Extracellular vesicles as drug delivery systems: Why and how?, Adv. Drug Deliv. Rev. 159 (2020) 332–343, https://doi.org/10.1016/j.addr.2020.04.004.
[11] D.E. Murphy, O.G. de Jong, M.J.W. Evers, M. Nurazizah, R.M. Schiffelers, P. Vader, Natural or Synthetic RNA Delivery: A Stoichiometric Comparison of Extracellular Vesicles and Synthetic Nanoparticles, Nano Lett. 21 (2021) 1888–1895, https://doi.org/10.1021/acs.nanolett.1c00094.
[12] E. Willms, C. Cabañas, I. Mäger, M.J.A. Wood, P. Vader, Extracellular vesicle heterogeneity: Subpopulations, isolation techniques, and diverse functions in cancer progression, Front. Immunol. 9 (2018), https://doi.org/10.3389/fimmu.2018.00738.
[13] T. Vagner, A. Chin, J. Mariscal, S. Bannykh, D.M. Engman, D. Di Vizio, Protein composition reflects extracellular vesicle heterogeneity, Proteomics 19 (2019) 1800167, https://doi.org/10.1002/pmic.201800167.
[14] C. Théry, K.W. Witwer, E. Aikawa, M.J. Alcaraz, J.D. Anderson, R. Andriantsitohaina, A. Antoniou, T. Arab, F. Archer, G.K. Atkin-Smith, D.C. Ayre, J.-M. Bach, D. Bachurski, H. Baharvand, L. Balaj, S. Baldacchino, N.N. Bauer, A.A. Baxter, M. Bebawy, C. Beckham, A. Bedina Zavec, A. Benmoussa, A.C. Berardi, P. Bergese, E. Bielska, C. Blenkiron, S. Bobis-Wozowicz, E. Boilard, W. Boireau, A. Bongiovanni, F.E. Borràs, S. Bosch, C.M. Boulanger, X. Breakefield, A.M. Breglio, M.Á. Brennan, D.R. Brigstock, A. Brisson, M.L. Broekman, J.F. Bromberg, P. Bryl-Górecka, S. Buch, A.H. Buck, D. Burger, S. Busatto, D. Buschmann, B. Bussolati, E.I. Buzás, J.B. Byrd, G. Camussi, D.R. Carter, S. Caruso, L.W. Chamley, Y.-T. Chang, C. Chen, S. Chen, L. Cheng, A.R. Chin, A. Clayton, S.P. Clerici, A. Cocks, E. Cocucci, R.J. Coffey, A. Cordeiro-da-Silva, Y. Couch, F.A. Coumans, B. Coyle, R. Crescitelli, M.F. Criado, C. D'Souza-Schorey, S. Das, A. Datta Chaudhuri, P. de Candia, E.F. De Santana, O. De Wever, H.A. Del Portillo, T. Demaret, S. Deville, A. Devitt, B. Dhondt, D. Di Vizio, L.C. Dieterich, V. Dolo, A.P. Dominguez Rubio, M. Dominici, M.R. Dourado, T.A. Driedonks, F. V Duarte, H.M. Duncan, R.M. Eichenberger, K. Ekström, S. El Andaloussi, C. Elie-Caille, U. Erdbrügger, J.M. Falcón-Pérez, F. Fatima, J.E. Fish, M. Flores-Bellver, A. Försönits, A. Frelet-Barrand, F. Fricke, G. Fuhrmann, S. Gabrielsson, A. Gámez-Valero, C. Gardiner, K. Gärtner, R. Gaudin, Y.S. Gho, B. Giebel, C. Gilbert, M. Gimona, I. Giusti, D.C. Goberdhan, A. Görgens, S.M. Gorski, D.W. Greening, J.C. Gross, A. Gualerzi, G.N. Gupta, D. Gustafson, A. Handberg, R.A. Haraszti, P. Harrison, H. Hegyesi, A. Hendrix, A. F. Hill, F.H. Hochberg, K.F. Hoffmann, B. Holder, H. Holthofer, B. Hosseinkhani, G. Hu, Y. Huang, V. Huber, S. Hunt, A.G.-E. Ibrahim, T. Ikezu, J.M. Inal, M. Isin, A. Ivanova, H.K. Jackson, S. Jacobsen, S.M. Jay, M. Jayachandran, G. Jenster, L. Jiang, S.M. Johnson, J.C. Jones, A. Jong, T. Jovanovic-Talisman, S. Jung, R. Kalluri, S.-I. Kano, S. Kaur, Y. Kawamura, E.T. Keller, D. Khamari, E. Khomyakova, A. Khvorova, P. Kierulf, K.P. Kim, T. Kislinger, M. Klingeborn, D.J. Klinke 2nd, M. Kornek, M.M. Kosanović, Á.F. Kovács, E.-M. Krämer-Albers, S. Krasemann, M. Krause, I. V Kurochkin, G.D. Kusuma, S. Kuypers, S. Laitinen, S.M. Langevin, L.R. Languino, J. Lannigan, C. Lässer, L.C. Laurent, G. Lavieu, E. Lázaro-Ibáñez, S. Le Lay, M.-S. Lee, Y.X.F. Lee, D.S. Lemos, M. Lenassi, A. Leszczynska, I.T. Li, K. Liao, S.F. Libregts, E. Ligeti, R. Lim, S.K. Lim, A. Linē, K. Linnemannstöns, A. Llorente, C.A. Lombard, M.J. Lorenowicz, Á.M. Lörincz, J. Lötvall, J. Lovett, M.C. Lowry, X. Loyer, Q. Lu, B. Lukomska, T.R. Lunavat, S.L. Maas, H. Malhi, A. Marcilla, J. Mariani, J. Mariscal, E.S. Martens-Uzunova, L. Martin-Jaular, M.C. Martinez, V.R. Martins, M. Mathieu, S. Mathivanan, M. Maugeri, L.K. McGinnis, M.J. McVey, D.G. Meckes Jr, K.L. Meehan, I. Mertens, V.R. Minciacchi, A. Möller, M. Møller Jørgensen, A. Morales-Kastresana, J. Morhayim, F. Mullier, M. Muraca, L. Musante, V. Mussack, D.C. Muth, K.H. Myburgh, T. Najrana, M. Nawaz, I. Nazarenko, P. Nejsum, C. Neri, T. Neri, R. Nieuwland, L. Nimrichter, J.P. Nolan, E.N. Nolte-'t Hoen, N. Noren Hooten, L. O'Driscoll, T. O'Grady, A. O'Loghlen, T. Ochiya, M. Olivier, A. Ortiz, L.A. Ortiz, X. Osteikoetxea, O. Østergaard, M. Ostrowski, J. Park, D.M. Pegtel, H. Peinado, F. Perut, M.W. Pfaffl, D.G. Phinney, B.C. Pieters, R.C. Pink, D.S. Pisetsky, E. Pogge von Strandmann, I. Polakovicova, I.K. Poon, B.H. Powell, I. Prada, L. Pulliam, P. Quesenberry, A. Radeghieri, R.L. Raffai, S. Raimondo, J. Rak, M.I. Ramirez, G. Raposo, M.S. Rayyan, N. Regev-Rudzki, F.L. Ricklefs, P.D. Robbins, D.D. Roberts, S.C. Rodrigues, E. Rohde, S. Rome, K.M. Rouschop, A. Rughetti, A.E. Russell, P. Saá, S. Sahoo, E. Salas-Huenuleo, C. Sánchez, J.A. Saugstad, M.J. Saul, R.M. Schiffelers, R. Schneider, T.H. Schøyen, A. Scott, E. Shahaj, S. Sharma, O. Shatnyeva, F. Shekari, G.V. Shelke, A.K. Shetty, K. Shiba, P.R.-M. Siljander, A.M. Silva, A. Skowronek, O.L. Snyder 2nd, R.P. Soares, B.W. Sódar, C. Soekmadji, J. Sotillo, P.D. Stahl, W. Stoorvogel, S.L. Stott, E.F. Strasser, S. Swift, H. Tahara, M. Tewari, K. Timms, S. Tiwari, R. Tixeira, M. Tkach, W.S. Toh, R. Tomasini, A.C. Torrecilhas, J.P. Tosar, V. Toxavidis, L. Urbanelli, P. Vader, B.W. van Balkom, S.G. van der Grein, J. Van Deun, M.J. van Herwijnen, K. Van Keuren-Jensen, G. van Niel, M.E. van Royen, A.J. van Wijnen, M.H. Vasconcelos, I.J. Vechetti Jr, T.D. Veit, L.J. Vella, É. Velot, F.J. Verweij, B. Vestad, J.L. Viñas, T. Visnovitz, K. V Vukman, J. Wahlgren, D.C. Watson, M.H. Wauben, A. Weaver, J.P. Webber, V. Weber, A.M. Wehman, D.J. Weiss, J.A. Welsh, S. Wendt, A.M. Wheelock, Z. Wiener, L. Witte, J. Wolfram, A. Xagorari, P. Xander, J. Xu, X. Yan, M. Yáñez-Mó, H. Yin, Y. Yuana, V. Zappulli, J. Zarubova, V. Žėkas, J.-Y. Zhang, Z. Zhao, L. Zheng, A.R. Zheutlin, A.M. Zickler, P. Zimmermann, A.M. Zivkovic, D. Zocco, E.K. Zuba-Surma, Minimal information for studies of extracellular vesicles 2018 (MISEV2018): a position statement of the International Society for Extracellular Vesicles and update of the MISEV2014 guidelines, J. Extracell. Vesicles. 7 (2018) 1535750. Doi: 10.1080/20013078.2018.1535750.
[15] J. Ratajczak, K. Miekus, M. Kucia, J. Zhang, R. Reca, P. Dvorak, M.Z. Ratajczak, Embryonic stem cell-derived microvesicles reprogram hematopoietic progenitors: Evidence for horizontal transfer of mRNA and protein delivery, Leukemia. 20 (2006) 847–856, https://doi.org/10.1038/sj.leu.2404132.
[16] H. Valadi, K. Ekström, A. Bossios, M. Sjöstrand, J.J. Lee, J.O. Lötvall, Exosome-mediated transfer of mRNAs and microRNAs is a novel mechanism of genetic exchange between cells, Nat. Cell Biol. 9 (2007) 654–659, https://doi.org/10.1038/ncb1596.
[17] S. El Andaloussi, I. Mäger, X.O. Breakefield, M.J.A. Wood, Extracellular vesicles: Biology and emerging therapeutic opportunities, Nat. Rev. Drug Discov. 12 (2013) 347–357, https://doi.org/10.1038/nrd3978.
[18] G. Van Niel, G. D'Angelo, G. Raposo, Shedding light on the cell biology of extracellular vesicles, Nat. Rev. Mol. Cell Biol. 19 (2018) 213–228, https://doi.org/10.1038/nrm.2017.125.
[19] L. Alvarez-Erviti, Y. Seow, H. Yin, C. Betts, S. Lakhal, M.J.A. Wood, Delivery of siRNA to the mouse brain by systemic injection of targeted exosomes, Nat. Biotechnol. 29 (2011) 341–345, https://doi.org/10.1038/nbt.1807.
[20] W.M. Usman, T.C. Pham, Y.Y. Kwok, L.T. Vu, V. Ma, B. Peng, Y.S. Chan, L. Wei, S. M. Chin, A. Azad, A.B.L. He, A.Y.H. Leung, M. Yang, N. Shyh-Chang, W.C. Cho, J. Shi, M.T.N. Le, Efficient RNA drug delivery using red blood cell extracellular vesicles, Nat. Commun. 9 (2018), https://doi.org/10.1038/s41467-018-04791-8.
[21] L. Zhao, C. Gu, Y. Gan, L. Shao, H. Chen, H. Zhu, Exosome-mediated siRNA delivery to suppress postoperative breast cancer metastasis, J. Control. Release. 318 (2020) 1–15, https://doi.org/10.1016/j.jconrel.2019.12.005.
[22] B. Mateescu, E.J.K. Kowal, B.W.M. van Balkom, S. Bartel, S.N. Bhattacharyya, E. I. Buzás, A.H. Buck, P. de Candia, F.W.N. Chow, S. Das, T.A.P. Driedonks, L. Fernández-Messina, F. Haderk, A.F. Hill, J.C. Jones, K.R. Van Keuren-Jensen, C. P. Lai, C. Lässer, I. di Liegro, T.R. Lunavat, M.J. Lorenowicz, S.L.N. Maas, I. Mäger, M. Mittelbrunn, S. Momma, K. Mukherjee, M. Nawaz, D.M. Pegtel, M. W. Pfaffl, R.M. Schiffelers, H. Tahara, C. Théry, J.P. Tosar, M.H.M. Wauben, K.W. Witwer, E.N.M. Nolte-'t Hoen, Obstacles and opportunities in the functional analysis of extracellular vesicle RNA – an ISEV position paper, J. Extracell. Vesicles. 6 (2017) 1286095, https://doi.org/10.1080/20013078.2017.1286095.
[23] D.E. Murphy, O.G. de Jong, M. Brouwer, M.J. Wood, G. Lavieu, R.M. Schiffelers, P. Vader, Extracellular vesicle-based therapeutics: natural versus engineered targeting and trafficking, Exp. Mol. Med. 51 (2019), https://doi.org/10.1038/s12276-019-0223-5.
[24] G.E. Melling, E. Carollo, R. Conlon, J.C. Simpson, D.R.F. Carter, The Challenges and Possibilities of Extracellular Vesicles as Therapeutic Vehicles, Eur. J. Pharm. Biopharm. 144 (2019) 50–56, https://doi.org/10.1016/j.ejpb.2019.08.009.
[25] D.B. Nguyen, T.B. Thuy Ly, M.C. Wesseling, M. Hittinger, A. Torge, A. Devitt, Y. Perrie, I. Bernhardt, Characterization of Microvesicles Released from Human Red Blood Cells, Cell. Physiol. Biochem. 38 (2016) 1085–1099, https://doi.org/10.1159/000443059.
[26] E. Willms, H.J. Johansson, I. Mäger, Y. Lee, K.E.M. Blomberg, M. Sadik, A. Alaarg, C.I.E. Smith, J. Lehtiö, S. El Andaloussi, M.J.A. Wood, P. Vader, Cells release subpopulations of exosomes with distinct molecular and biological properties, Sci. Rep. 6 (2016), https://doi.org/10.1038/srep22519.
[27] S. Kaur, A.G. Elkahloun, A. Arakelyan, L. Young, T.G. Myers, F. Otaizo-Carrasquero, W. Wu, L. Margolis, D.D. Roberts, CD63, MHC class 1, and CD47 identify subsets of extracellular vesicles containing distinct populations of noncoding RNAs, Sci. Rep. 8 (2018), https://doi.org/10.1038/s41598-018-20936-7.
[28] Z. Wei, A.O. Batagov, S. Schinelli, J. Wang, Y. Wang, R. El Fatimy, R. Rabinovsky, L. Balaj, C.C. Chen, F. Hochberg, B. Carter, X.O. Breakefield, A.M. Krichevsky, Coding and noncoding landscape of extracellular RNA released by

human glioma stem cells, Nat. Commun. 8 (2017) 1145, https://doi.org/10.1038/s41467-017-01196-x.
[29] E.N.M. Nolte-'t Hoen, H.P.J. Buermans, M. Waasdorp, W. Stoorvogel, M.H.M. Wauben, P.A.C. 't Hoen, Deep sequencing of RNA from immune cell-derived vesicles uncovers the selective incorporation of small non-coding RNA biotypes with potential regulatory functions, Nucleic Acids Res. 40 (2012) 9272–9285, https://doi.org/10.1093/nar/gks658.
[30] K. O'Brien, K. Breyne, S. Ughetto, L.C. Laurent, X.O. Breakefield, RNA delivery by extracellular vesicles in mammalian cells and its applications, Nat. Rev. Mol. Cell Biol. 21 (2020) 585–606, https://doi.org/10.1038/s41580-020-0251-y.
[31] J.R. Chevillet, Q. Kang, I.K. Ruf, H.A. Briggs, L.N. Vojtech, S.M. Hughes, H.H. Cheng, J.D. Arroyo, E.K. Meredith, E.N. Gallichotte, E.L. Pogosova-Agadjanyan, C. Morrissey, D.L. Stirewalt, F. Hladik, E.Y. Yu, C.S. Higano, M. Tewari, Quantitative and stoichiometric analysis of the microRNA content of exosomes, Proc. Natl. Acad. Sci. U. S. A. 111 (2014) 14888–14893, https://doi.org/10.1073/pnas.1408301111.
[32] S.T.-Y. Chuo, J.C.-Y. Chien, C.P.-K. Lai, Imaging extracellular vesicles: current and emerging methods, J. Biomed. Sci. 25 (2018) 91, https://doi.org/10.1186/s12929-018-0494-5.
[33] T. Nolan, R.E. Hands, S.A. Bustin, Quantification of mRNA using real-time RT-PCR, Nat. Protoc. 1 (2006) 1559–1582, https://doi.org/10.1038/nprot.2006.236.
[34] J.P. Levesque-Sergerie, M. Duquette, C. Thibault, L. Delbecchi, N. Bissonnette, Detection limits of several commercial reverse transcriptase enzymes: Impact on the low- and high-abundance transcript levels assessed by quantitative RT-PCR, BMC Mol. Biol. 8 (2007) 93, https://doi.org/10.1186/1471-2199-8-93.
[35] B.J. Hindson, K.D. Ness, D.A. Masquelier, P. Belgrader, N.J. Heredia, A.J. Makarewicz, I.J. Bright, M.Y. Lucero, A.L. Hiddessen, T.C. Legler, T.K. Kitano, M. R. Hodel, J.F. Petersen, P.W. Wyatt, E.R. Steenblock, P.H. Shah, L.J. Bousse, C.B. Troup, J.C. Mellen, D.K. Wittmann, N.G. Erndt, T.H. Cauley, R.T. Koehler, A.P. So, S. Dube, K.A. Rose, L. Montesclaros, S. Wang, D.P. Stumbo, S.P. Hodges, S. Romine, F.P. Milanovich, H.E. White, J.F. Regan, G.A. Karlin-Neumann, C.M. Hindson, S. Saxonov, B.W. Colston, High-throughput droplet digital PCR system for absolute quantitation of DNA copy number, Anal. Chem. 83 (2011) 8604–8610, https://doi.org/10.1021/ac202028g.
[36] K. Takahashi, I.K. Yan, C. Kim, J. Kim, T. Patel, Analysis of extracellular RNA by digital PCR, Front. Oncol. 4 (2014) 129, https://doi.org/10.3389/fonc.2014.00129.
[37] C. Wang, Q. Ding, P. Plant, M. Basheer, C. Yang, E. Tawedrous, A. Krizova, C. Boulos, M. Farag, Y. Cheng, G.M. Yousef, Droplet digital PCR improves urinary exosomal miRNA detection compared to real-time PCR, Clin. Biochem. 67 (2019) 54–59, https://doi.org/10.1016/j.clinbiochem.2019.03.008.
[38] K.R. Kukurba, S.B. Montgomery, RNA sequencing and analysis, Cold Spring Harb. Protoc. 2015 (2015) 951–969, https://doi.org/10.1101/pdb.top084970.
[39] Z. Wei, A.O. Batagov, D.R.F. Carter, A.M. Krichevsky, Fetal Bovine Serum RNA Interferes with the Cell Culture derived Extracellular RNA, Sci. Rep. 6 (2016) 31175, https://doi.org/10.1038/srep31175.
[40] M. Auber, D. Fröhlich, O. Drechsel, E. Karaulanov, E.-M. Krämer-Albers, Serum-free media supplements carry miRNAs that co-purify with extracellular vesicles, J. Extracell. Vesicles. 8 (2019) 1656042, https://doi.org/10.1080/20013078.2019.1656042.
[41] S. Bala, T. Csak, F. Momen-Heravi, D. Lippai, K. Kodys, D. Catalano, A. Satishchandran, V. Ambros, G. Szabo, Biodistribution and function of extracellular miRNA-155 in mice, Sci. Rep. 5 (2015) 1–12, https://doi.org/10.1038/srep10721.
[42] J. Wahlgren, T.L. De Karlson, M. Brisslert, F. Vaziri Sani, E. rn Telemo, P. Sunnerhagen, H. Valadi, Plasma exosomes can deliver exogenous short interfering RNA to monocytes and lymphocytes, Nucleic Acids Res. 40 (2012) e130. Doi: 10.1093/nar/gks463.
[43] Z. Yang, J. Xie, J. Zhu, C. Kang, C. Chiang, X. Wang, X. Wang, T. Kuang, F. Chen, Z. Chen, A. Zhang, B. Yu, R.J. Lee, L. Teng, L.J. Lee, Functional exosome-mimic for delivery of siRNA to cancer: in vitro and in vivo evaluation, J. Control. Release. 243 (2016) 160–171, https://doi.org/10.1016/j.jconrel.2016.10.008.
[44] Q. Li, Y. Kim, J. Namm, A. Kulkarni, G.R. Rosania, Y.H. Ahn, Y.T. Chang, RNA-selective, live cell imaging probes for studying nuclear structure and function, Chem. Biol. 13 (2006) 615–623, https://doi.org/10.1016/j.chembiol.2006.04.007.
[45] Y.J. Lu, Q. Deng, D.P. Hu, Z.Y. Wang, B.H. Huang, Z.Y. Du, Y.X. Fang, W.L. Wong, K. Zhang, C.F. Chow, A molecular fluorescent dye for specific staining and imaging of RNA in live cells: A novel ligand integration from classical thiazole orange and styryl compounds, Chem. Commun. 51 (2015) 15241–15244, https://doi.org/10.1039/c5cc05551b.
[46] J. Mighty, J. Zhou, A. Benito-Martin, S. Sauma, S. Hanna, O. Onwumere, C. Shi, M. Muntzel, M. Sauane, M. Young, H. Molina, D. Cox, S. Redenti, Analysis of adult neural retina extracellular vesicle release, RNA transport and proteomic cargo 30-30 Investig. Ophthalmol. Vis. Sci. 61 (2020), https://doi.org/10.1167/iovs.61.2.30.
[47] M. Li, E. Zeringer, T. Barta, J. Schageman, A. Cheng, A.V. Vlassov, Analysis of the RNA content of the exosomes derived from blood serum and urine and its potential as biomarkers, Philos. Trans. R. Soc. B Biol. Sci. 369 (2014), https://doi.org/10.1098/rstb.2013.0502.
[48] S. Tyagi, F.R. Kramer, Molecular Beacons: Probes that Fluoresce Upon Hybridization, Nat. Biotechnol. 14 (1996) 303–308, https://doi.org/10.1038/nbt0396-303.
[49] J.H. Lee, J.A. Kim, M.H. Kwon, J.Y. Kang, W.J. Rhee, In situ single step detection of exosome microRNA using molecular beacon, Biomaterials. 54 (2015) 116–125, https://doi.org/10.1016/j.biomaterials.2015.03.014.
[50] W.J. Rhee, S. Jeong, Extracellular Vesicle miRNA Detection Using Molecular Beacons, in: Methods Mol. Biol. , Humana Press, New York, 2017: pp. 287–294. Doi: 10.1007/978-1-4939-7253-1_23.
[51] J.H. Lee, J.A. Kim, S. Jeong, W.J. Rhee, Simultaneous and multiplexed detection of exosome microRNAs using molecular beacons, Biosens. Bioelectron. 86 (2016) 202–210, https://doi.org/10.1016/j.bios.2016.06.058.
[52] D.S. Peabody, The RNA binding site of bacteriophage MS2 coat protein, EMBO J. 12 (1993) 595–600, https://doi.org/10.1002/j.1460-2075.1993.tb05691.x.
[53] D. Fusco, N. Accornero, B. Lavoie, S.M. Shenoy, J.M. Blanchard, R.H. Singer, E. Bertrand, Single mRNA molecules demonstrate probabilistic movement in living mammalian cells, Curr. Biol. 13 (2003) 161–167, https://doi.org/10.1016/S0960-9822(02)01436-7.
[54] C.P. Lai, E.Y. Kim, C.E. Badr, R. Weissleder, T.R. Mempel, B.A. Tannous, X.O. Breakefield, Visualization and tracking of tumour extracellular vesicle delivery and RNA translation using multiplexed reporters, Nat. Commun. 6 (2015) 7029, https://doi.org/10.1038/ncomms8029.
[55] J.G.J. Bauman, J. Wiegant, P. Borst, P. van Duijn, A new method for fluorescence microscopical localization of specific DNA sequences by in situ hybridization of fluorochrome-labelled RNA, Exp. Cell Res. 128 (1980) 485–490, https://doi.org/10.1016/0014-4827(80)90087-7.
[56] E.D. Pastuzyn, C.E. Day, R.B. Kearns, M. Kyrke-Smith, A.V. Taibi, J. McCormick, N. Yoder, D.M. Belnap, S. Erlendsson, D.R. Morado, J.A.G. Briggs, C. Feschotte, J. D. Shepherd, The neuronal gene arc encodes a repurposed retrotransposon gag protein that mediates intercellular RNA transfer, Cell. 172 (2018) 275–288.e18, https://doi.org/10.1016/j.cell.2017.12.024.
[57] A.M. Femino, F.S. Fay, K. Fogarty, R.H. Singer, Visualization of single RNA transcripts in situ, New Ser. 280 (1998) 585–590.
[58] A. Raj, P. van den Bogaard, S.A. Rifkin, A. van Oudenaarden, S. Tyagi, Imaging individual mRNA molecules using multiple singly labeled probes, Nat. Methods. 5 (2008) 877–879, https://doi.org/10.1038/nmeth.1253.
[59] G. Haimovich, J.E. Gerst, Detection of mRNA transfer between mammalian cells in coculture by single-molecule fluorescent in situ hybridization (smFISH), in: Methods Mol. Biol., Humana Press Inc., 2019: pp. 109–129. Doi: 10.1007/978-1-4939-9674-2_8.
[60] K.M. Kim, K. Abdelmohsen, M. Mustapic, D. Kapogiannis, M. Gorospe, RNA in extracellular vesicles, Wiley Interdiscip. Rev. RNA. 8 (2017), https://doi.org/10.1002/wrna.1413 e1413.
[61] J. Kersigo, N. Pan, J.D. Lederman, S. Chatterjee, T. Abel, G. Pavlinkova, I. Silos-Santiago, B. Fritzsch, A RNAscope whole mount approach that can be combined with immunofluorescence to quantify differential distribution of mRNA, Cell Tissue Res. 374 (2018) 251–262, https://doi.org/10.1007/s00441-018-2864-4.
[62] M. Omerzu, N. Fenderico, B. De Barbanson, J. Sprangers, J. De Ridder, M.M. Maurice, Three-dimensional analysis of single molecule FISH in human colon organoids, Biol. Open. 8 (2019), https://doi.org/10.1242/bio.042812.
[63] S. Wang, Single molecule RNA FISH (smFISH) in whole-mount mouse embryonic organs, Curr. Protoc. Cell Biol. 83 (2019), https://doi.org/10.1002/cpcb.79.
[64] M.P. Gupta, S. Tandalam, S. Ostrager, A.S. Lever, A.R. Fung, D.D. Hurley, G.B. Alegre, J.E. Espinal, H.L. Remmel, S. Mukherjee, B.M. Levine, R.P. Robins, H. Molina, B.D. Dill, C.M. Kenific, T. Tuschl, D. Lyden, D.J. D'Amico, J.T.G. Pena, Non-reversible tissue fixation retains extracellular vesicles for in situ imaging, Nat. Methods. 16 (2019) 1269–1273, https://doi.org/10.1038/s41592-019-0623-4.
[65] H.M.T. Choi, J.Y. Chang, L.A. Trinh, J.E. Padilla, S.E. Fraser, N.A. Pierce, Programmable in situ amplification for multiplexed imaging of mRNA expression, Nat. Biotechnol. 28 (2010) 1208–1212, https://doi.org/10.1038/nbt.1692.
[66] P. Zhuang, H. Zhang, R.M. Welchko, R.C. Thompson, S. Xu, D.L. Turner, Combined microRNA and mRNA detection in mammalian retinas by in situ hybridization chain reaction, Sci. Rep. 10 (2020), https://doi.org/10.1038/s41598-019-57194-0.
[67] F. Wang, J. Flanagan, N. Su, L.C. Wang, S. Bui, A. Nielson, X. Wu, H.T. Vo, X.J. Ma, Y. Luo, RNAscope: A novel in situ RNA analysis platform for formalin-fixed, paraffin-embedded tissues, J. Mol. Diagnostics. 14 (2012) 22–29, https://doi.org/10.1016/j.jmoldx.2011.08.002.
[68] C. Larsson, I. Grundberg, O. Söderberg, M. Nilsson, In situ detection and genotyping of individual mRNA molecules, Nat. Methods. 7 (2010) 395–397, https://doi.org/10.1038/nmeth.1448.
[69] C. Lin, M. Jiang, S. Duan, J. Qiu, Y. Hong, X. Wang, X. Chen, R. Ke, Visualization of individual microRNA molecules in fixed cells and tissues using target-primed padlock probe assay, Biochem. Biophys. Res. Commun. 526 (2020) 607–611, https://doi.org/10.1016/j.bbrc.2020.03.134.
[70] E. Lubeck, L. Cai, Single-cell systems biology by super-resolution imaging and combinatorial labeling, Nat. Methods. 9 (2012) 743–748, https://doi.org/10.1038/nmeth.2069.
[71] J.M. Levsky, S.M. Shenoy, R.C. Pezo, R.H. Singer, Single-cell gene expression profiling, Science (80-.). 297 (2002) 836–840. Doi: 10.1126/science.1072241.
[72] J.H. Lee, E.R. Daugharthy, J. Scheiman, R. Kalhor, T.C. Ferrante, R. Terry, B.M. Turczyk, J.L. Yang, H.S. Lee, J. Aach, K. Zhang, G.M. Church, Fluorescent in situ sequencing (FISSEQ) of RNA for gene expression profiling in intact cells and tissues, Nat. Protoc. 10 (2015) 442–458, https://doi.org/10.1038/nprot.2014.191.

[73] J.R. Moffitt, X. Zhuang, RNA Imaging with Multiplexed Error-Robust Fluorescence in Situ Hybridization (MERFISH), in: Methods Enzymol., Academic Press Inc., 2016: pp. 1–49. Doi: 10.1016/bs.mie.2016.03.020.
[74] K.H. Chen, A.N. Boettiger, J.R. Moffitt, S. Wang, X. Zhuang, Spatially resolved, highly multiplexed RNA profiling in single cells, Science (80-.) (2015) 348, https://doi.org/10.1126/science.aaa6090.
[75] C. Xia, H.P. Babcock, J.R. Moffitt, X. Zhuang, Multiplexed detection of RNA using MERFISH and branched DNA amplification, Sci. Rep. 9 (2019), https://doi.org/10.1038/s41598-019-43943-8.
[76] C. Xia, J. Fan, G. Emanuel, J. Hao, X. Zhuang, Spatial transcriptome profiling by MERFISH reveals subcellular RNA compartmentalization and cell cycle-dependent gene expression, Proc. Natl. Acad. Sci. U. S. A. 116 (2019) 19490–19499, https://doi.org/10.1073/pnas.1912459116.
[77] E. Lubeck, A.F. Coskun, T. Zhiyentayev, M. Ahmad, L. Cai, Single-cell in situ RNA profiling by sequential hybridization, Nat. Methods. 11 (2014) 360–361, https://doi.org/10.1038/nmeth.2892.
[78] G. Wang, J.R. Moffitt, X. Zhuang, Multiplexed imaging of high-density libraries of RNAs with MERFISH and expansion microscopy, Sci. Rep. 8 (2018), https://doi.org/10.1038/s41598-018-22297-7.
[79] C.H.L. Eng, M. Lawson, Q. Zhu, R. Dries, N. Koulena, Y. Takei, J. Yun, C. Cronin, C. Karp, G.C. Yuan, L. Cai, Transcriptome-scale super-resolved imaging in tissues by RNA seqFISH+, Nature. 568 (2019) 235–239, https://doi.org/10.1038/s41586-019-1049-y.
[80] J.J.L. Goh, N. Chou, W.Y. Seow, N. Ha, C.P.P. Cheng, Y.-C. Chang, Z.W. Zhao, K.H. Chen, Highly specific multiplexed RNA imaging in tissues with split-FISH, Nat. Methods. 17 (2020) 689–693, https://doi.org/10.1038/s41592-020-0858-0.
[81] D.P. Bratu, B.J. Cha, M.M. Mhlanga, F.R. Kramer, S. Tyagi, Visualizing the distribution and transport of mRNAs in living cells, Proc. Natl. Acad. Sci. U. S. A. 100 (2003) 13308–13313, https://doi.org/10.1073/pnas.2233244100.
[82] A.K. Chen, M.A. Behlke, A. Tsourkas, Efficient cytosolic delivery of molecular beacon conjugates and flow cytometric analysis of target RNA, Nucleic Acids Res. 36 (2008), https://doi.org/10.1093/nar/gkn331 e69.
[83] B. Turner-Bridger, M. Jakobs, L. Muresan, H.H.W. Wong, K. Franze, W.A. Harris, C.E. Holt, Single-molecule analysis of endogenous β-actin mRNA trafficking reveals a mechanism for compartmentalized mRNA localization in axons, Proc. Natl. Acad. Sci. U. S. A. 115 (2018) E9697–E9706, https://doi.org/10.1073/pnas.1806189115.
[84] E. Corradi, I. Dalla Costa, A. Gavoci, A. Iyer, M. Roccuzzo, T.A. Otto, E. Oliani, S. Bridi, S. Strohbuecker, G. Santos-Rodriguez, D. Valdembri, G. Serini, C. Abreu-Goodger, M. Baudet, Axonal precursor miRNA s hitchhike on endosomes and locally regulate the development of neural circuits, EMBO J. (2020) 1–24, https://doi.org/10.15252/embj.2019102513.
[85] C. Chen, S. Zong, Z. Wang, J. Lu, D. Zhu, Y. Zhang, R. Zhang, Y. Cui, Visualization and intracellular dynamic tracking of exosomes and exosomal miRNAs using single molecule localization microscopy, Nanoscale. 10 (2018) 5154–5162, https://doi.org/10.1039/c7nr08800k.
[86] G.P. de Oliveira, E. Zigon, G. Rogers, D. Davodian, S. Lu, T. Jovanovic-Talisman, J. Jones, J. Tigges, S. Tyagi, I.C. Ghiran, Detection of Extracellular Vesicle RNA Using Molecular Beacons, IScience. 23 (2020), https://doi.org/10.1016/j.isci.2019.100782.
[87] K.E. Bauer, I. Segura, I. Gaspar, V. Scheuss, C. Illig, G. Ammer, S. Hutten, E. Basyuk, S.M. Fernández-Moya, J. Ehses, E. Bertrand, M.A. Kiebler, Live cell imaging reveals 3′-UTR dependent mRNA sorting to synapses, Nat. Commun. 10 (2019) 1–13, https://doi.org/10.1038/s41467-019-11123-x.
[88] B. Wu, J. Chen, R.H. Singer, Background free imaging of single mRNAs in live cells using split fluorescent proteins, Sci. Rep. 4 (2014) 3615, https://doi.org/10.1038/srep03615.
[89] J. Wu, S. Zaccara, D. Khuperkar, H. Kim, M.E. Tanenbaum, S.R. Jaffrey, Live imaging of mRNA using RNA-stabilized fluorogenic proteins, Nat. Methods. 16 (2019) 862–865, https://doi.org/10.1038/s41592-019-0531-7.
[90] E. Charpentier, J.A. Doudna, Biotechnology: Rewriting a genome, Nature. 495 (2013) 50–51, https://doi.org/10.1038/495050a.
[91] M.R. O'Connell, B.L. Oakes, S.H. Sternberg, A. East-Seletsky, M. Kaplan, J.A. Doudna, Programmable RNA recognition and cleavage by CRISPR/Cas9, Nature. 516 (2014) 263–266, https://doi.org/10.1038/nature13769.
[92] D.A. Nelles, M.Y. Fang, M.R. O'Connell, J.L. Xu, S.J. Markmiller, J.A. Doudna, G. W. Yeo, Programmable RNA Tracking in Live Cells with CRISPR/Cas9, Cell. 165 (2016) 488–496, https://doi.org/10.1016/j.cell.2016.02.054.
[93] M.E. Tanenbaum, L.A. Gilbert, L.S. Qi, J.S. Weissman, R.D. Vale, A protein-tagging system for signal amplification in gene expression and fluorescence imaging, Cell. 159 (2014) 635–646, https://doi.org/10.1016/j.cell.2014.09.039.
[94] N.-H. Sun, D.-Y. Chen, L.-P. Ye, G. Sheng, J.-J. Gong, B.-H. Chen, Y.-M. Lu, F. Han, CRISPR-Sunspot: Imaging of endogenous low-abundance RNA at the single-molecule level in live cells, Theranostics. 10 (2020) 10993–11012, https://doi.org/10.7150/thno.43094.
[95] O.O. Abudayyeh, J.S. Gootenberg, P. Essletzbichler, S. Han, J. Joung, J.J. Belanto, V. Verdine, D.B.T. Cox, M.J. Kellner, A. Regev, E.S. Lander, D.F. Voytas, A.Y. Ting, F. Zhang, RNA targeting with CRISPR-Cas13, Nature. 550 (2017) 280–284, https://doi.org/10.1038/nature24049.
[96] S.C. Strutt, R.M. Torrez, E. Kaya, O.A. Negrete, J.A. Doudna, RNA-dependent RNA targeting by CRISPR-Cas9, Elife. 7 (2018), https://doi.org/10.7554/eLife.32724 e32724.
[97] L.-Z. Yang, Y. Wang, S.-Q. Li, R.-W. Yao, P.-F. Luan, H. Wu, G.G. Carmichael, L.-L. Chen, Dynamic Imaging of RNA in Living Cells by CRISPR-Cas13 Systems, Mol. Cell. 76 (2019) 981–997.e7, https://doi.org/10.1016/j.molcel.2019.10.024.
[98] J.S. Paige, K.Y. Wu, S.R. Jaffrey, RNA mimics of green fluorescent protein, Science (80-.). 333 (2011) 642–646. Doi: 10.1126/science.1207339.
[99] G.S. Filonov, J.D. Moon, N. Svensen, S.R. Jaffrey, Broccoli: rapid selection of an RNA mimic of green fluorescent protein by fluorescence-based selection and directed evolution, J. Am. Chem. Soc. 136 (2014) 16299–16308, https://doi.org/10.1021/ja508478x.
[100] E.V. Dolgosheina, S.C.Y. Jeng, S.S.S. Panchapakesan, R. Cojocaru, P.S.K. Chen, P. D. Wilson, N. Hawkins, P.A. Wiggins, P.J. Unrau, RNA Mango aptamer-fluorophore: A bright, high-affinity complex for RNA labeling and tracking, ACS Chem. Biol. 9 (2014) 2412–2420, https://doi.org/10.1021/cb500499x.
[101] X. Chen, D. Zhang, N. Su, B. Bao, X. Xie, F. Zuo, L. Yang, H. Wang, L. Jiang, Q. Lin, M. Fang, N. Li, X. Hua, Z. Chen, C. Bao, J. Xu, W. Du, L. Zhang, Y. Zhao, L. Zhu, J. Loscalzo, Y. Yang, Visualizing RNA dynamics in live cells with bright and stable fluorescent RNAs, Nat. Biotechnol. 37 (2019) 1287–1293, https://doi.org/10.1038/s41587-019-0249-1.
[102] F. Bouhedda, K.T. Fam, M. Collot, A. Autour, S. Marzi, A. Klymchenko, M. Ryckelynck, A dimerization-based fluorogenic dye-aptamer module for RNA imaging in live cells, Nat. Chem. Biol. 16 (2020) 69–76, https://doi.org/10.1038/s41589-019-0381-8.
[103] E. Braselmann, A.J. Wierzba, J.T. Polaski, M. Chromiński, Z.E. Holmes, S.T. Hung, D. Batan, J.R. Wheeler, R. Parker, R. Jimenez, D. Gryko, R.T. Batey, A.E. Palmer, A multicolor riboswitch-based platform for imaging of RNA in live mammalian cells, Nat. Chem. Biol. 14 (2018) 964–971, https://doi.org/10.1038/s41589-018-0103-7.
[104] A.D. Cawte, P.J. Unrau, D.S. Rueda, Live cell imaging of single RNA molecules with fluorogenic Mango II arrays, Nat. Commun. 11 (2020) 1283, https://doi.org/10.1038/s41467-020-14932-7.
[105] H. Ma, L.-C. Tu, A. Naseri, Y.-C. Chung, D. Grunwald, S. Zhang, T. Pederson, CRISPR-Sirius: RNA scaffolds for signal amplification in genome imaging, Nat. Methods. 15 (2018) 928–931, https://doi.org/10.1038/s41592-018-0174-0.
[106] N. Kikuchi, D.M. Kolpashchikov, Split Spinach Aptamer for Highly Selective Recognition of DNA and RNA at Ambient Temperatures, ChemBioChem. 17 (2016) 1589–1592, https://doi.org/10.1002/cbic.201600323.
[107] K.K. Alam, K.D. Tawiah, M.F. Lichte, D. Porciani, D.H. Burke, A Fluorescent Split Aptamer for Visualizing RNA-RNA Assembly in Vivo, ACS Synth. Biol. 6 (2017) 1710–1721, https://doi.org/10.1021/acssynbio.7b00059.
[108] Z. Wang, Y. Luo, X. Xie, X. Hu, H. Song, Y. Zhao, J. Shi, L. Wang, G. Glinsky, N. Chen, R. Lal, C. Fan, In situ spatial complementation of aptamer-mediated recognition enables live-cell imaging of native RNA transcripts in real time, Angew. Chemie - Int. Ed. 57 (2018) 972–976, https://doi.org/10.1002/anie.201707795.
[109] A.P.K.K. Karunanayake Mudiyanselage, Q. Yu, M.A. Leon-Duque, B. Zhao, R. Wu, M. You, Genetically encoded catalytic hairpin assembly for sensitive RNA imaging in live cells, J. Am. Chem. Soc. 140 (2018) 8739–8745, https://doi.org/10.1021/jacs.8b03956.
[110] A. Zomer, S.C. Steenbeek, C. Maynard, J. Van Rheenen, Studying extracellular vesicle transfer by a Cre-loxP method, Nat. Protoc. 11 (2016) 87–101, https://doi.org/10.1038/nprot.2015.138.
[111] F. de la Cuesta, I. Passalacqua, J. Rodor, R. Bhushan, L. Denby, A.H. Baker, Extracellular vesicle cross-talk between pulmonary artery smooth muscle cells and endothelium during excessive TGF-β signalling: implications for PAH vascular remodelling, Cell Commun. Signal. 17 (2019) 143, https://doi.org/10.1186/s12964-019-0449-9.
[112] K. Ridder, S. Keller, M. Dams, A.-K. Rupp, J. Schlaudraff, Extracellular vesicle-mediated transfer of genetic information between the hematopoietic system and the brain in response to inflammation, PLoS Biol. 12 (2014) 1001874, https://doi.org/10.1371/journal.pbio.1001874.
[113] K. Ridder, A. Sevko, J. Heide, M. Dams, A.K. Rupp, J. Macas, J. Starmann, M. Tjwa, K.H. Plate, H. Sültmann, P. Altevogt, V. Umansky, S. Momma, Extracellular vesicle-mediated transfer of functional RNA in the tumor microenvironment, Oncoimmunology. 4 (2015), https://doi.org/10.1080/2162402X.2015.1008371.
[114] X. Yan, T.A. Hoek, R.D. Vale, M.E. Tanenbaum, Dynamics of Translation of Single mRNA Molecules in Vivo, Cell. 165 (2016) 976–989, https://doi.org/10.1016/j.cell.2016.04.034.
[115] O.G. de Jong, D.E. Murphy, I. Mäger, E. Willms, A. Garcia-Guerra, J.J. Gitz-Francois, J. Lefferts, D. Gupta, S.C. Steenbeek, J. van Rheenen, S. El Andaloussi, R.M. Schiffelers, M.J.A. Wood, P. Vader, A CRISPR-Cas9-based reporter system for single-cell detection of extracellular vesicle-mediated functional transfer of RNA, Nat. Commun. 11 (2020) 1113, https://doi.org/10.1038/s41467-020-14977-8.
[116] K. Huang, F. Demirci, M. Batish, W. Treible, B.C. Meyers, J.L. Caplan, Quantitative, super-resolution localization of small RNAs with sRNA-PAINT, Nucleic Acids Res. 48 (2020), https://doi.org/10.1093/nar/gkaa623 e96.
[117] F. Chen, A.T. Wassie, A.J. Cote, A. Sinha, S. Alon, S. Asano, E.R. Daugharthy, J.B. Chang, A. Marblestone, G.M. Church, A. Raj, E.S. Boyden, Nanoscale imaging of RNA with expansion microscopy, Nat. Methods. 13 (2016) 679–684, https://doi.org/10.1038/nmeth.3899.